

กรณีวัตถุประสงค์ประกอบสำหรับการบำบัดสารหนูในน้ำบาดาล



นางสาวปวีณา กิจบุตรวัฒน์

จุฬาลงกรณ์มหาวิทยาลัย

CHULALONGKORN UNIVERSITY

บทคัดย่อและแฟ้มข้อมูลฉบับเต็มของวิทยานิพนธ์ตั้งแต่ปีการศึกษา 2554 ที่ให้บริการในคลังปัญญาจุฬาฯ (CUIR)

เป็นแฟ้มข้อมูลของนิสิตเจ้าของวิทยานิพนธ์ ที่ส่งผ่านทางบัณฑิตวิทยาลัย

The abstract and full text of theses from the academic year 2011 in Chulalongkorn University Intellectual Repository (CUIR)

are the thesis authors' files submitted through the University Graduate School.

วิทยานิพนธ์นี้เป็นส่วนหนึ่งของการศึกษาตามหลักสูตรปริญญาวิทยาศาสตรมหาบัณฑิต

สาขาวิชาธรณีวิทยา ภาควิชาธรณีวิทยา

คณะวิทยาศาสตร์ จุฬาลงกรณ์มหาวิทยาลัย

ปีการศึกษา 2559

ลิขสิทธิ์ของจุฬาลงกรณ์มหาวิทยาลัย

COMPOSITE GEOLOGICAL MATERIALS FOR TREATMENT OF ARSENIC IN GROUNDWATER

Miss Paveena Kitbutrawat



A Thesis Submitted in Partial Fulfillment of the Requirements
for the Degree of Master of Science Program in Geology

Department of Geology

Faculty of Science

Chulalongkorn University

Academic Year 2016

Copyright of Chulalongkorn University

Thesis Title	COMPOSITE GEOLOGICAL MATERIALS FOR TREATMENT OF ARSENIC IN GROUNDWATER
By	Miss Paveena Kitbutrawat
Field of Study	Geology
Thesis Advisor	Waruntorn Kantipanyacharoen, Ph.D.
Thesis Co-Advisor	Seelawut Damrongsiri, Ph.D.

Accepted by the Faculty of Science, Chulalongkorn University in Partial
Fulfillment of the Requirements for the Master's Degree

..... Dean of the Faculty of Science
(Associate Professor Polkit Sangvanich, Ph.D.)

THESIS COMMITTEE

..... Chairman
(Professor Montri Choowong, Ph.D.)

..... Thesis Advisor
(Waruntorn Kantipanyacharoen, Ph.D.)

..... Thesis Co-Advisor
(Seelawut Damrongsiri, Ph.D.)

..... Examiner
(Associate Professor Chakkaphan Sutthirat, Ph.D.)

..... External Examiner
(Tawatchai Chualaowanich, Ph.D.)

ปวีณา กิจบุตราววัฒน์ : ธรณีวัสดุเชิงประกอบสำหรับการบำบัดสารหนูในน้ำบาดาล (COMPOSITE GEOLOGICAL MATERIALS FOR TREATMENT OF ARSENIC IN GROUNDWATER) อ.ที่ปรึกษาวิทยานิพนธ์หลัก: ดร. วรวิทย์ คณิตปัญญาเจริญ, อ.ที่ปรึกษาวิทยานิพนธ์ร่วม: ดร. ศีลาจตุร ดำรงค์ศิริ, 94 หน้า.

การปนเปื้อนสารหนูในน้ำบาดาลเป็นปัญหาสำคัญที่พบได้ในหลายประเทศ เนื่องจากการนำน้ำบาดาลที่มีการปนเปื้อนสารหนูมาใช้ในการอุปโภคและบริโภค ซึ่งก่อให้เกิดโรคร้ายแรงต่างๆ เช่น ไข้ดำ มะเร็งผิวหนัง โรคระบบประสาท โรคระบบทางเดินหายใจ และโรคเบาหวาน แม้ว่าในปัจจุบันมีการศึกษาวิธีการบำบัดสารหนูในน้ำบาดาลอย่างแพร่หลาย แต่ในประเทศไทยมีการศึกษาวิธีการบำบัดสารหนูในน้ำบาดาลไม่มากนัก งานวิจัยนี้จึงมุ่งเน้นศึกษาลักษณะทางเคมีและทางกายภาพที่สำคัญของหินและแร่ในท้องถิ่น เพื่อนำมาสร้างเป็นธรณีวัสดุเชิงประกอบที่สามารถดูดซับและบำบัดสารหนูออกจากแหล่งน้ำบาดาลได้อย่างมีประสิทธิภาพ

จากการศึกษาพบว่า ตัวดูดซับที่มีประสิทธิภาพสูง มีอัตราส่วนระหว่างหินทรายแป้งต่อหินเพอไลต์ที่ผ่านการเผาต่อดิน เป็น 66.67 ต่อ 16.67 ต่อ 16.67 ซึ่งเป็นตัวดูดซับที่มีรูพรุนสูง และสามารถคงรูปในน้ำได้ดี เมื่อนำตัวดูดซับไปทดสอบกับน้ำที่มีสารหนูปนเปื้อนในสภาวะต่างๆ พบว่าตัวดูดซับจำนวน 10 กรัม สามารถดูดซับสารหนูจากสารละลายที่มีสารหนูปนเปื้อนอยู่ 100 ไมโครกรัมต่อลิตร ปริมาณสารละลาย 50 มิลลิลิตรได้ดีที่สุด เมื่อค่าความเป็นกรดต่างของสารละลายอยู่ในระดับ 7 และแช่ตัวดูดซับเป็นเวลา 2 ชั่วโมง ซึ่งสารหนูสามารถถูกดูดซับออกไปได้สูงถึงร้อยละ 41.39 นอกจากนี้ข้อมูลที่ได้จากการทดลองถูกนำไปศึกษาหาเกลือที่จะอธิบายการดูดซับ โดยจากการคำนวณด้วยสมการการดูดซับแบบฟลินด์ซ พบว่า ค่าที่แสดงถึงความเป็นเนื้อเดียวกันของตัวดูดซับ มีค่าสูงถึง 1.27 ซึ่งแสดงว่าเกลือในการดูดซับเป็นแบบซับซ้อน ต่อมาในการคำนวณด้วยสมการการดูดซับของคูบิน-ราตซ์เควิช พบว่าค่าพลังงานในการดูดซับมีค่าเท่ากับ 3.79 กิโลจูลต่อโมล ซึ่งแสดงว่าการดูดซับเป็นแบบกายภาพ และในการประมาณค่าการดูดซับสารหนูสูงสุดจากสมการแบบแลงมัวร์ มีค่าเท่ากับ 0.45 มิลลิกรัมต่อตัวดูดซับ 1 กรัม

จากการทดลองใช้ตัวดูดซับกับตัวอย่างน้ำบาดาลที่ปนเปื้อนสารหนูจากบ่อบาดาลจำนวน 11 บ่อ ในพื้นที่อำเภอด่านช้าง จังหวัดสุพรรณบุรี และอำเภอบ้านไร่ จังหวัดอุทัยธานี ที่มีปริมาณสารหนู 16.13 ถึง 362.30 ไมโครกรัมต่อลิตร และมีค่าความเป็นกรดต่างประมาณ 6.95 ถึง 7.35 พบว่าสารหนูถูกดูดซับไปร้อยละ 20.17 ถึง 75.31 เมื่อใช้ตัวดูดซับ 10 กรัมต่อน้ำบาดาล 50 มิลลิลิตร เป็นเวลา 2 ชั่วโมง ซึ่งสาเหตุที่ตัวดูดซับทำงานด้วยประสิทธิภาพที่แตกต่างกันในแต่ละพื้นที่ คือปริมาณฟอสเฟตที่ละลายอยู่ในน้ำบาดาลที่ อาจมีผลต่อการดูดซับสารหนู เนื่องจากมีลักษณะโครงสร้างใกล้เคียงกับอาร์เซนไนต์ซึ่งเป็นสารประกอบของสารหนู และปริมาณธาตุแมกนีเซียมที่หลุดออกมาจากตัวดูดซับ ซึ่งทำให้ประสิทธิภาพการดูดซับสารหนูลดลง

ภาควิชา ธรณีวิทยา

สาขาวิชา ธรณีวิทยา

ปีการศึกษา 2559

ลายมือชื่อนิสิต

ลายมือชื่อ อ.ที่ปรึกษาหลัก

ลายมือชื่อ อ.ที่ปรึกษาร่วม

5772052523 : MAJOR GEOLOGY

KEYWORDS: ARSENIC / CONTAMINATION / GROUNDWATER / EXPANDED PERLITE

PAVEENA KITBUTRAWAT: COMPOSITE GEOLOGICAL MATERIALS FOR TREATMENT OF ARSENIC IN GROUNDWATER. ADVISOR: WARUNTORN KANTIPANYACHAROEN, Ph.D., CO-ADVISOR: SEELAWUT DAMRONGSIRI, Ph.D., 94 pp.

Arsenic contamination in groundwater is an important problem in many countries and responsible for many life-threatening diseases such as black fever, cancer, neurological and cardiovascular diseases, and diabetes. Despite the proposal of several remediation techniques worldwide, it has been challenging to find a cost-effective method to remove arsenic from groundwater in Thailand. This research is thus aimed to study chemical and physical properties of geological materials to create cost-effective adsorbents for arsenic removal.

The most effective adsorbent is made of porous siltstone, expanded perlite, and soil sample at the ratio of 66.67 to 16.67 to 16.67, respectively. The adsorbents are tested with arsenic contaminated water at different conditions and suggest that the most suitable condition is to use 10 grams of adsorbents per 50 ml of adsorbate at the pH of 7 with 2 hours of contact time. This experimental condition can remove arsenic up to 41.39%. Experimental results are further used in Freundlich, Dubinin – Radushkevich, and Langmuir equations to understand the adsorption behaviors. The value of $1/n$ from Freundlich adsorption isotherm is 1.27, indicating that the surface of adsorbent is heterogeneous. The energy of sorption from Dubinin – Radushkevich adsorption isotherm is 3.79 kJ/mol, suggesting the kinetic is physical adsorption. In addition, the maximum capacity of adsorbent from Langmuir adsorption isotherm is 0.45 mg/g.

Adsorbents are further tested with natural groundwater from 11 wells in Amphoe Dan Chang, Suphan Buri and Amphoe Ban Rai, Uthai Thani which contain arsenic ranges from 16.13 to 362.3 $\mu\text{g/l}$ and have pH ranges from 6.95 to 7.35. After submerging 10 grams of adsorbents into 50 ml of contaminated groundwater for 2 hours, arsenic can be effectively removed between 20.17% and 75.31%. The variable amount of arsenic removal is likely due to the presence of phosphate, which has a similar structure to arsenite. In addition, the disintegration of adsorbents may release a noticeable amount of magnesium, which in turn inhibits the adsorption of arsenic and decreases the arsenic removal percentage.

Department: Geology

Field of Study: Geology

Academic Year: 2016

Student's Signature

Advisor's Signature

Co-Advisor's Signature

ACKNOWLEDGEMENTS

The autor would like to express sincere thanks to Dr.Waruntorn Kanitpanyacharoen, thesis advisor and Dr.Seelawut Damrongsiri, thesis co-advisor. The growth of many ideas in this thesis was greatly facilitated by discussion with them. In addition, I am also grateful to Professor Dr.Montri Choowong, Associate Professor Dr.Chakkaphan Sutthirat and Dr.Tawatchai Chualaowanich, the thesis committee for their guidances, encouragement, and critical reading the thesis.

Grateful acknowledgement are due to Mrs.Kannikar Medhanavyn, Miss Pekultong Prasertsak, Mrs.Onuma Khamphlaeng, Miss Suwimon Janewongpaisan, and Mrs.Saowanee Sieammai, Department of Mineral Resources for providing many invaluable and creative suggestions.

Grateful acknowledgement are also to the staffs of Department of Geology, Chulalongkorn University, for helping in laboratory.

Finally, I would like to thank ma parent, my sisters, and my brother for their encouragement and support throughout the study.

CONTENTS

	Page
THAI ABSTRACT	iv
ENGLISH ABSTRACT	v
ACKNOWLEDGEMENTS	vi
CONTENTS	vii
LIST OF TABLES	xi
LIST OF FIGURES	xiii
CHAPTER I.....	1
INTRODUCTION.....	1
1.1 Objective.....	7
1.2 Scope	7
1.3 Expected outputs.....	7
CHAPTER II.....	8
LITERATURE REVIEWS	8
2.1 Theory.....	8
2.1.1 Theory of adsorption	8
2.1.2 Theory of equilibrium adsorption isotherm	10
2.2 Literature reviews.....	12
2.2.1 Reviews of diatomaceous earth	12
2.2.3 Reviews of other geological material	16
CHAPTER III.....	18
METHODOLOGY.....	18
3.1 Adsorbent preparations	18

	Page
3.1.1 X-ray Diffraction (XRD).....	19
3.1.2 Wavelength Dispersive X-ray Fluorescence (WDXRF).....	20
3.1.3 Mix and mold the adsorbents.....	21
3.1.4 Pore and surface of adsorbents.....	22
3.1.5 Cation exchange capacity (CEC).....	23
3.2. Adsorption capacity test.....	24
3.3 Adsorbent testing in Natural Contaminated Groundwater.....	27
CHAPTER IV.....	29
RESULTS.....	29
4.1 Adsorbents preparation.....	29
4.1.1 Composition of geomaterials.....	29
4.1.2 Mold adsorbent.....	34
4.1.4 Cation exchange capacity (CEC).....	42
4.2 Adsorption efficiency.....	42
4.2.1 Scenario 1 : effect of adsorbent dose.....	42
4.2.2 Scenario 2 : effect of contact time.....	44
4.2.3 Scenario 3 : effect of concentration of As.....	45
4.2.4 Scenario 4 : effect of pH.....	46
4.2.5 Scenario 5: effect of pH (As concentration 50 ppb).....	47
4.2.6 Scenario 6: effect of contact time after adjusting the pH contaminated water to 7.....	48
4.2.7 Scenario 7 : effect of As concentration after adjusting the pH to 7.....	50
4.3 Adsorbent testing in natural contaminated groundwater.....	52

	Page
CHAPTER V	56
DISCUSSION.....	56
5.1 The adsorption mechanism	56
5.2 The Adsorption Isotherm.....	58
5.2.1 Langmuir Adsorption Isotherm.....	58
5.2.2 Freundlich Adsorption Isotherm	60
5.2.3 The Dubinin – Radushkevich Adsorption Isotherm.....	62
5.3 The comparison of maximum capacity, specific surface area, and cation exchange capacity of adsorbent.....	64
5.4 The discussion about the arsenic removal from groundwater.....	65
CHAPTER VI	72
CONCLUSION	72
6.1 Conclusions	72
6.2 Recommendation for future studies.....	73
REFERENCES	74
VITA.....	94

LIST OF TABLES

Tables	Page
Table 3.1 : Mixture Design of 3 components (by weight percent)	22
Table 3.2 : A summary of conditions used in adsorption capacity test.	25
Table 4.1 : The oxide composition of siltstone (weight percent) analyzed by XRF.....	30
Table 4.2 : The oxide composition of expanded perlite (weight percent) analyzed by XRF.....	32
Table 4.3 : The oxide composition of soil sample (weight percent) analyzed by XRF.....	33
Table 4.4 : The oxide composition of adsorbent type 12 (weight percent) analyzed by XRF.....	40
Table 4.5 : The variation of adsorbent amount.....	43
Table 4.6: The variation of contact time.....	44
Table 4.7 : The variation of concentration (C_0).....	45
Table 4.8 : The variation of pH for As concentration is 50 ppb.	46
Table 4.9 : The variation of pH for As concentration is 100 ppb.	48
Table 4.10 : The variation of contact time at pH equal to 7.....	49
Table 4.11 : The variation of concentration at pH equal to 7.....	51
Table 4.12 : The sampling point and some properties of groundwater sample.	52
Table 4.13 : The concentrations of cation and anion in groundwater sample before and after treatment. Treated sample is in italic and marked with an asterisk sign (*).	53
Table 4.14 : The percentages of arsenic removal in groundwater samples after treating with geo-adsorbents.....	54

Tables	Page
Table 5.1 : The As concentration of the initial solution (C_0) and the As concentration after equilibrium (C_e) and the amount of As adsorbed (q_e).	57
Table 5.2 : Parameters used in Langmuir Adsorption Isotherm calculation	59
Table 5.3 : Results from Langmuir Adsorption Isotherm.....	60
Table 5.4 : Parameters used in Freundlich Adsorption Isotherm calculation.....	61
Table 5.5 : Results from Freundlich Adsorption Isotherm.....	62
Table 5.6 : Parameters used in Dubinin – Radushkevich Adsorption Isotherm calculation.	63
Table 5.7 : Results from Dubinin-Radushkevich Adsorption Isotherm.	64
Table 5.8 : A comparison between maximum capacity, specific surface area, and cation exchange capacity of adsorbent.....	65
Table 5.9 : Arsenic and phosphate removal percentages.	69
Table 5.10 : The result of arsenic removal percentage and potassium increasing percentage.	70

LIST OF FIGURES

Figures	Page
Figure 1.1: A map of diatomite distribution in Lampang.....	4
Figure 1.2 : A map of perlite distribution at Lopburi.....	5
Figure 1.3 : A map of kaolin distribution in Amphoe Chae Hom, Lampang.....	6
Figure 2.1 : A graph of solid-liquid coefficient.....	9
Figure 2.2 : A scanning Electron Microscopy (SEM) image of diatomite type 1	13
Figure 2.3 : A SEM image of diatomite type 2.	14
Figure 2.4 : A SEM image of diatomite type 3.	14
Figure 2.5 A XRD diffractogram of (A) non-treated expanded perlite and (B) base treated perlite. Red spectrum is 3 hours reflux and blue spectrum is 5 hours reflux.	16
Figure 3.1 : Geomaterials used to make the adsorbents. (A) siltstone, (B) soil sample, and (C) expanded perlite.	19
Figure 3.2 : A diagram of X-ray Diffraction method.	20
Figure 3.3 : A diagram of the operating system of X-Ray Fluorescence	20
Figure 3.4 : A trilinear coordinate system from Minitab suggesting mixture design of adsorbents 3 components of degree 3.	21
Figure 3.5 : A diagram of the operating system of SEM (after Department of.....	23
Figure 3.6 : A diagram of Graphite Furnace Atomic Absorption Spectroscopy (GFAAS).....	26
Figure 3.7 : A diagram of Inductively Coupled Plasma Optical Emission Spectrometry (ICP-OES).....	27
Figure 4.1 : A X-ray diffraction pattern of siltstone.....	29
Figure 4.2 : A SEM image of siltstone.	30

Figures	Page
Figure 4.3: A X-ray diffraction pattern of expanded perlite.....	31
Figure 4.4 : A X-ray diffraction pattern of soil sample sample.	33
Figure 4.5 : The adsorbent type 1.....	34
Figure 4.6 : The adsorbent type 2.....	34
Figure 4.7 : The adsorbent type 3.....	35
Figure 4.8 : The adsorbent type 4.....	35
Figure 4.9 : The adsorbent type 5.....	35
Figure 4.10 : The adsorbent type 6.....	36
Figure 4.11 : The adsorbent type 7.....	36
Figure 4.12 : The adsorbent type 8.....	37
Figure 4.13 : The adsorbent type 9.....	37
Figure 4.14 : The adsorbent type 10.	37
Figure 4.15 : The adsorbent type 11.	38
Figure 4.16 : The adsorbent type 12.	38
Figure 4.17 : The adsorbent type 13.	38
Figure 4.18: A dissolution of the adsorbents after puts in the water. Adsorbent type 12 (A) being still constant, and Adsorbent type 2 (B) is the representation of the tender types.	39
Figure 4.19 : A X-ray diffraction pattern of adsorbent type 12.	40
Figure 4.20 : A X-ray diffraction pattern of adsorbent type 12.	41
Figure 4.21 : A SEM image of porous structure of the unheated adsorbent.	41
Figure 4.22: A SEM image of small porous structure of the heated adsorbent.	42
Figure 4.23 : Arsenic removal percentage as a function of the amount of the adsorbent added.	43

Figures	Page
Figure 4.24 : Arsenic removal percentage as a function of the contact time.....	45
Figure 4.25 : Arsenic removal percentage as a function of the concentration.....	46
Figure 4.26 : Arsenic removal by varying pH value.	47
Figure 4.27 : Arsenic removal by varying pH value.	48
Figure 4.28 : Arsenic removal percentage as a function of the contact time.....	50
Figure 4.29 : Arsenic removal percentage as a function of the concentration.....	51
Figure 4.30 : The comparison of the initial As concentration and the remaining As concentration after treatment.....	55
Figure 5.1: A graph of solid – liquid distribution coefficient.	57
Figure 5.2 : A graph of Langmuir Adsorption Isotherm.	59
Figure 5.3 : A graph of Freundlich Adsorption Isotherm.....	61
Figure 5.4 : A graph of Dubinin-Radushkevich Adsorption Isotherm.....	63
Figure 5.5 : The effect of pH on the adsorbent.	66
Figure 5.6 : The dominant As (III) species in the solution is controlled by pH.....	67
Figure 5.7 : The dominant As (V) species in the solution is controlled by pH.....	67
Figure 5.8 : Molecular structure of phosphate (left) and arsenate (right).....	68
Figure 5.9 : The various species of phosphate in the solution is controlled by pH.....	68
Figure 5.10 : A graph of arsenic removal percentages and the changes of potassium volumes.....	71

CHAPTER I

INTRODUCTION

Arsenic contaminated groundwater is a leading environmental problem in many countries, particularly in the United States of America, Bangladesh, Nepal, Vietnam, Taiwan, China, South Korea, Japan, and Thailand (Mukherjee et al., 2006). High intake of arsenic leads to life-threatening diseases such as black fever, cancer, neurological and cardiovascular diseases, and diabetes (Smedley and Kinniburgh, 2005). Naturally occurring arsenic often arises in rock formations with high volumes of arsenopyrite (FeAsS) and other sulfide minerals. Arsenic is considered a metalloid and found in many oxidation states, of which arsenic (III) and arsenic (V) being the most common. In Thailand, arsenic contaminated groundwater has been reported in some parts of Amphoe Ron Phibun in Nakorn Si Thammarat (Bavornsachoti, 1995), and arsenic contaminated surface water has been reported in Amphoe Dan Chang in Suphan Buri (Bureau of Mineral Resources Identification and Research, 2013) and Amphoe Banrai in Uthai Thani (Bureau of Mineral Resources Identification and Research, 2014). While the causes of arsenic occurrence in these areas involve long-term comprehensive studies, the removal of arsenic contaminants in groundwater requires immediate remediation methods. This study thus aims to investigate physical and chemical properties of different geomaterials which can be used to make adsorbents for arsenic removal from groundwater.

Heavy metal contamination in groundwater is a worldwide problem. When heavy metals are exposed to rain or surface water resources, they can readily combine with oxygen and form metal compounds in water. Contaminated water can further percolate along cracks or faults, reaching the groundwater system, and largely impact human and other living organisms. Most commonly occurred metal contaminants include lead (Pb), cadmium (Cd), chromium (Cr), zinc (Zn), mercury (Hg), copper (Cu), and arsenic (As). Arsenic is a metalloid with the atomic number of 33. It occurs in various arsenic-bearing mineral such as orpiment (As_2S_3), realgar (As_4S_4), arsenopyrite (FeAsS) and scorodite ($FeAsO_4 \cdot 2H_2O$) associated with metal ore deposits. In addition, inorganic arsenic compounds can be separated into two groups. The first group forming as arsenite (As(III)), or trivalent compounds such as As_2O_3 , $NaAsO_2$, AsH_3 , $AsCl_3$, and

As_2O_3 , occurring in a reduction phase. The As-rich rocks are normally weathered in basic environments. As (III) is mobilable in water and may precipitate as a contaminant within layers of alluvial sediments. At pH 0 to pH 9, arsenite is formed as H_3AsO_3 , which is a non-polar compound. At pH > 9, arsenite can be formed as H_2AsO_3^- and HAsO_3^{2-} , which have negative polarity. The second group forming as arsenate (As (V)), or pentavalent compounds such as As_2O_5 and H_3AsO_4 , are existing in an oxidation phase. In an acid environment, As (V) generally exists and spreads to a large area. In a basic environment, As (V) is normally precipitated with iron oxide and aluminium oxide. At pH 0 to pH 2, arsenate is formed as H_3AsO_4 , which is a non-polar form. At pH > 2, arsenate is formed as H_2AsO_4^- , HAsO_4^{2-} , and AsO_4^{2-} , which have negative polarity (Jiang et al., 2013).



Arsenic is widely used in industries for making extremely hard metal alloy material, paint pigments, and agricultural applications. A high amount of arsenic is naturally found in various rock formations; for example Neogene - Quaternary volcanic deposits associated with post-volcanic geysers and thermal spring in Argentina, lower Mekong basin in Cambodia, and the Red River in Vietnam. Arsenic contamination caused by anthropogenic activities were also found in many countries such as Australia, Brazil, Bulgaria, Canada, Chile, China, Czech, Germany, Greece, India, Japan, Mexico, Spain, Sweden, Thailand, and United of Kingdom. Anthropogenic sources include mineral mining, metal smelting, coal burning, agriculture and wastewater from factories (Mukherjee et al., 2006). In Thailand, people living in the vicinity of some tin mines have been suffered from black fever, skin cancer, bronchial cancer, urinary cancer, and leukemia; for example, in Amphoe Ron Phibun in Nakorn Si Thammarat (Bavornsachoti, 1995). The others area, which found the As contaminated in groundwater are Prachuap Khiri Khan, Yala, Uthai Thani, Suphan Buri, Ranong, Phangnga, Phuket, Chiang Mai, Chumphon, Amphoe Khun Yuam in Mae Hong Son, Amphoe Mae Ramat in Tak, Amphoe Thong Pha Phum in Kanchanaburi, Amphoe Suan Phueng in Ratchaburi and Andaman coastal (Athikom-rangsarit, 1994).

To prevent the spreading of arsenic related diseases, the remediation techniques for arsenic contaminants have been proposed such as bio-remediation, physical-remediation, and chemical-remediation with pump and treat technique, pumps water to the water tank and puts adsorbents or chemical solvents to the tanks to remove the contaminants (Ahmed, 2001). The bio-remediation is mainly used in

contaminated soils by cropping some plants such as banana and calendula to decrease the concentration of arsenic in soil (Nakwanit, 2010). The toxic substance is accumulated in roots and trunks, but not found in leaves and fruits. In addition, bacteria such as *Gallionella ferrunginea* and *Leptothrix ochracea* can be used to remove more than 80% from the initial As (III) concentration (Katsoyiannis et al., 2002). Examples of chemical treatment methods are electron-beam irradiation, mercury extraction, radiocolloid treatment, and removal by sorption (Barakat, 2011).

One of the geo-remediation techniques is to use geomaterials to make adsorbents for arsenic removal from groundwater. Geomaterial adsorbents are relatively cheaper than others methods. Geomaterials such as zeolite, goethite, and clay minerals have been studied and used to decrease the effect of arsenic contamination (Branislava et al., 2011). The most widely-used adsorbent is iron and manganese coated sand. For the initial As (III) concentrations of 50 µg/L and 300 µg/L, the coated sand can remove arsenic more than 90% and 50%, respectively (Ramaswami et al., 2001). This method is nontoxic and inexpensive (0.60 USD for water 3,650 liters). A study by Jalil and Ahmed (2001) further suggests that using activated alumina as adsorbents can effectively remove arsenic contaminants of more than 90%, but it is an expensive method (25.60 USD. for one time). The activated alumina can remove iron, cadmium, antimony, lead and uranium as well. Zeolite can remove as much as 75% of arsenic from contaminated water (Elizalde-Gonzalez et al., 2001). Other geological materials such as kaolinite and illite can remove both of As(III) and As(V), but require a long contact time at least 12 - 16 hours (Manning and Goldberg, 1997). Iron rich material, such as goethite and laterite that can remove arsenic as much as 95% (Sharmin, 2001) and 50-90% (Matis et al., 1999), respectively.

In addition, Ingleshoppe et al. (1999) uses diatomite as an alternative geomaterial adsorbent. Diatomite or diatomaceous earth is made of amorphous silica shells of diatoms. Diatomite is a sedimentary rock formed by the accumulation of diatom in lacustrine or marine sediments. Its fresh color is pale yellow to pale brown and weathering color is brown. Specific gravity is approximately 2 – 2.25 and the hardness is 5 - 6. Diatomite has high porosity, dull luster, and opaque. Diatomite in

Thailand found in Amphoe Mueang, Amphoe Koh Kha, Amphoe Mae Tha, and Amphoe Sop Prap in Lampang as shown in Figure 1.1. Diatomite in Lampang was deposited in Neogene basin. The price of diatomite is 900 baht per metric ton announced on 9 September 1980 (Department of Primary Industries and Mines Thailand, 2017). The abundance of diatomite in Thailand presents a plausible alternative material used as adsorbent for treating arsenic contaminated water. This study thus aims to explore the different properties of diatomite in combination with other geomaterial such as perlite and kaolin as key components for making geomaterial adsorbents.

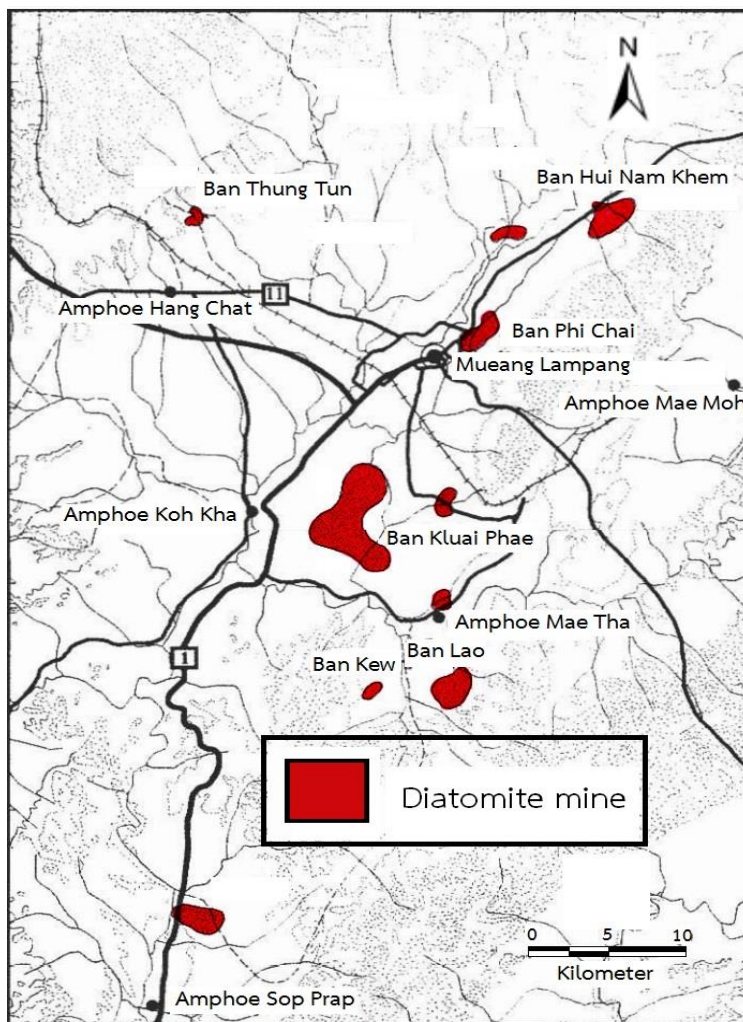


Figure 1.1: A map of diatomite distribution in Lampang (after Department of Mineral Resources Thailand, 2007).

Perlite is commonly used in water as filter (Mostafa et al., 2011). It is a very fine-grained and amorphous material formed during volcanic eruption. Perlite is green to black and its weathering color is pale gray. Specific gravity is approximately 2.3 – 2.8 and the hardness is 5.5 - 7. It contains mainly silica and water. When heated, the volume of original perlite can be expanded 5-20 times. Perlite is relatively light in weight, highly porous, and has high heat resistance. Perlite mines in Thailand are in Amphoe Sa Bot and Amphoe Khok Charoen in Lop buri as shown in Figure 1.2. The price of perlite is 1,500 baht per metric ton announced on 13 November 2015 (Department of Primary Industries and Mines Thailand, 2017).

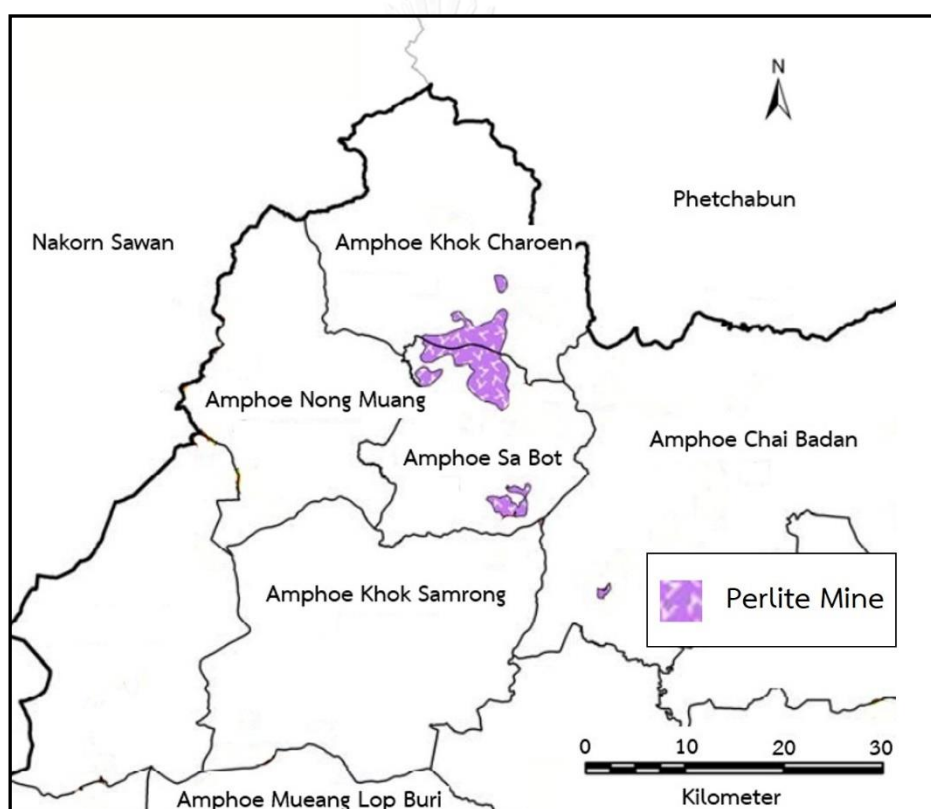


Figure 1.2 : A map of perlite distribution at Lopburi (after Saisutthichai, 2006 and Premmanee and Wijitchareampong, 1997).

A study by Manning and Goldberg (1997) suggests kaolin as a good geomaterial for making adsorbent. Kaolin contains mainly quartz, kaolinite, and others clay minerals. It is a very fine-grained mineral commonly used in ceramics industry and has

high ductility and high toughness. Its fresh color is white, but may have various colors due to the amount of trace element. Specific gravity is approximately 2.6 – 2.65 and the hardness is 2 – 2.5. In Thailand, kaolin is formed due to the weathering process of feldspar-rich volcanic rocks such as rhyolite, rhyolitic tuff and granite. Kaolin deposits are found in Chiang Mai, Lamphun, Lampang, Tak, Sukhothai, Phrae, Uttaradit, Uthai Thani, Kanchanaburi, Lop Buri, Prachin Buri, Rayong, Ratchaburi, Phichit, Nakhon Si Thammarat, Surat Thani, Chumphon, Ranong, Phangnga, Phuket, Songkhla, Yala and Narathiwat (Department Mineral Resources Thailand, 2017). The material source of kaolin used in this study is from Amphoe Chae Hom in Lampang (Figure 1.3). The price of filler grade is 1,900 baht per metric ton announced on 17 October 1994 (Department of Primary Industries and Mines Thailand, 2017).

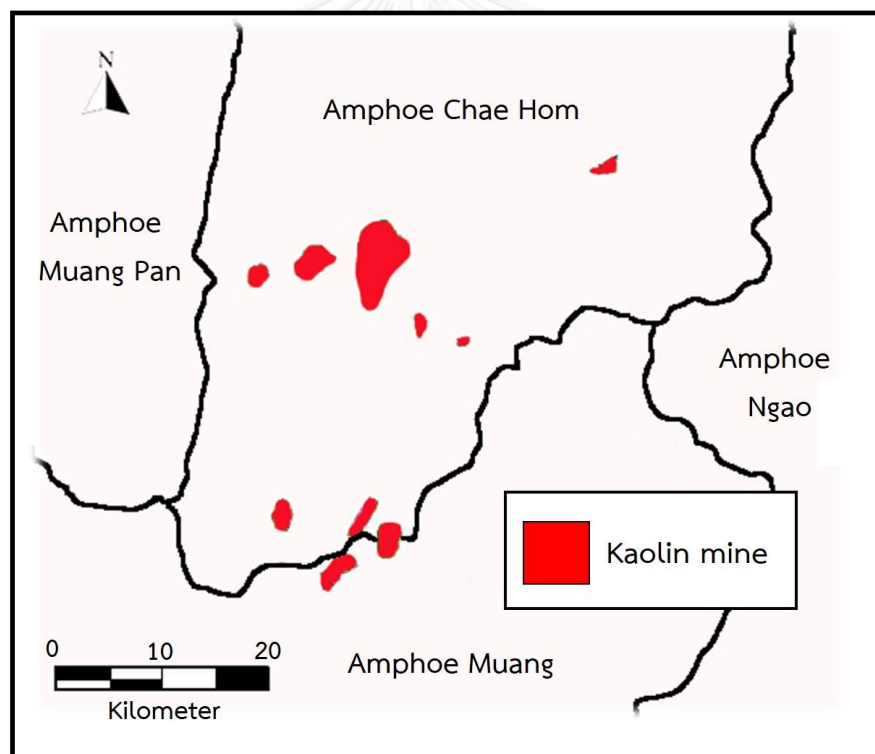


Figure 1.3 : A map of kaolin distribution in Amphoe Chae Hom, Lampang (after Department of Mineral Resources Thailand, 2007).

1.1 Objective

1.1.1 To investigate physical and chemical properties of geomaterial combination used to make adsorbent or adsorbent for arsenic contaminant removal from groundwater.

1.1.2 To determine suitable conditions for using adsorbents.

1.2 Scope

This thesis is focused on As(III) removal using geomaterial-combination adsorbents, which is composed of diatomite from Amphoe Mueang Lampang, expanded perlite from Amphoe Sa Bot, Lopburi, and kaolin from Amphoe Chae Hom, Lampang. The composition and volumes of different geomaterials are varied in order to create the most stable and cost-effective dsorbent. The adsorbent is also heated at 700°C for 3 hours in furnace to enhance the durability in water. The adsorbent is tested with natural and synthetic arsenic contaminated water samples. Synthetic contaminated water, which used in laboratory is made from diluted As(III) from As(III) standard solution 1000 ppm. Natural groundwater samples are collected from 11 wells in Amphoe Dan Chang, Suphan Buri and Amphoe Ban Rai,Uthai Thani.

1.3 Expected outputs

1.3.1 Obtain a low cost adsorbent for arsenic removal from contaminated groundwater resources.

1.3.2 Understand suitable conditions and the efficiency of using geomaterial adsorbents for arsenic removal.

CHAPTER II

LITERATURE REVIEWS

This chapter introduces previous studies on the theory of adsorption and different geomaterial used as adsorbents for groundwater treatment, particularly physical and chemical properties as well as origin and distribution of perlite, kaolin and diatomite.

2.1 Theory

2.1.1 Theory of adsorption

Adsorption is the interaction between atoms, ions, or molecules of gas or liquid to the solid surface, by making the film of gas or liquid on the surface of adsorbent. The adsorption is classified into two types. The first type is physical adsorption or physisorption, is caused by van der Waals force. Physical adsorption uses low energy, adsorb in multiple layers, and the reaction is reversible. The van der Waals force is described as a dipole – dipole force, which is the interaction between two permanent electromagnetism molecules, dipole – induced dipole which is the interaction between one electromagnetism molecule and the non-polar molecules, and London force which is the process between two non-polar molecules. The second type is chemical adsorption or chemisorption, which is caused by covalent bonding, high energy (20-100 Kcal/mol), adsorbed on monolayer, because the structure or chemical composition of adsorbent surface is reacted to adsorbate, and the reaction is irreversible (Noble and Terry, 2004).

According to Weber and Chakravorti (1974), the relationship between adsorbent and adsorbate can be explained by the solid-liquid coefficient graph (Figure 2.1), and use Equation 2.1 to calculated amount of metal adsorbed. The favorable and very favorable lines refer to when the adsorbent is suitable for adsorbate. Unfavorable isotherm means the adsorption is reversible.

$$q_e = \frac{(C_0 - C_e) \times V}{m}$$

Equation 2.1

Where:

C_0 = Concentration of As in the initial solution ($\mu\text{g/L}$)

C_e = Concentration of As after equilibrium ($\mu\text{g/L}$)

q_e = Amount of metal adsorbed (mg/g)

K = Solid – liquid distribution coefficient

V = Volume (l)

m = mass (kg.)

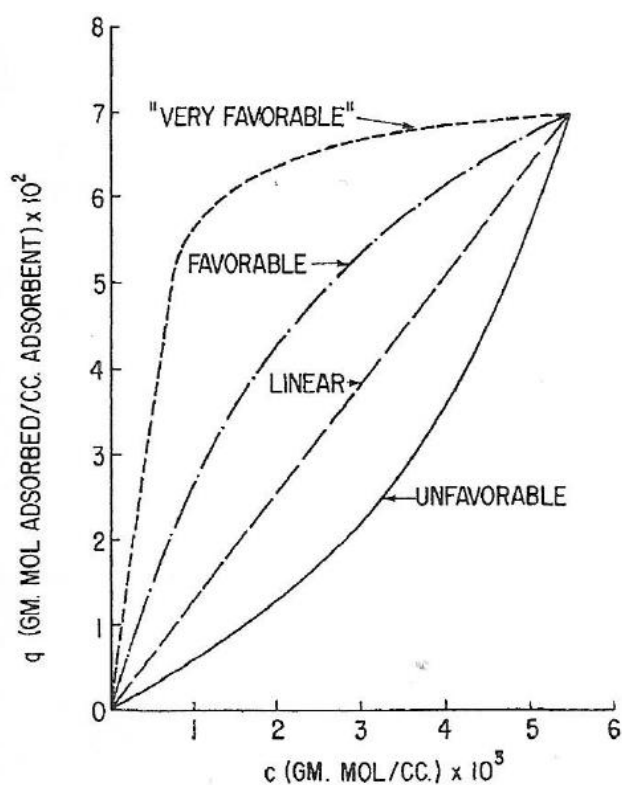


Figure 2.1 : A graph of solid-liquid coefficient.

2.1.2 Theory of equilibrium adsorption isotherm

The equilibrium adsorption isotherm describes the mechanism of adsorption. In generally, Langmuir adsorption isotherm and Freundlich adsorption isotherm are used to explain the adsorption.

Langmuir adsorption isotherm is the ideal of adsorption. It is used to describes the mechanism of adsorption, where the surface of the adsorbent is a perfectly flat plain and homogeneous. The adsorbent can adsorb one element on to monolayer, and do not have interaction between adsorbate molecules. Langmuir adsorption isotherm is also written as Equation 2.2, and the maximum capacity and Langmuir isotherm constant are calculated from the graph of Langmuir adsorption isotherm.

$$\frac{1}{q_e} = \frac{1}{Q_0} + \frac{1}{Q_0 K_L C_e} \quad \text{Equation 2.2}$$

$$R_L = \frac{1}{[1 + (1 + K_L C_0)]} \quad \text{Equation 2.3}$$

Where :

C_0 = Concentration in the initial solution (mg/L)

C_e = Concentration after equilibrium (mg/L)

q_e = Amount of metal adsorbed per gram of the adsorbent at equilibrium (mg/g)

Q_0 = Maximum capacity (mg/g)

K_L = Langmuir isotherm constant (L/mg)

$\frac{1}{Q_0 K_L}$ = Slope of a graph

V = Volume (l)

m = mass (kg.)

R_L = The mechanism adsorption

R_L value indicates the mechanism adsorption. If R_L is more than 1, the mechanism adsorption is unfavorable. If R_L is 1, the mechanism adsorption is linear. If R_L ranges between 0 and 1, the mechanism adsorption is favorable. Moreover, if R_L is 0, the mechanism adsorption is irreversible.

Freundlich adsorption isotherm is used to describe the mechanism of adsorption, where the surface of the adsorbent is heterogeneous. The adsorbent can adsorb more than one layer, and the adsorbate molecules are interact to the adsorbents. Freundlich adsorption isotherm is also written as Equation 2.4, and the function of the strength of adsorption process ($1/n$) and Freundlich isotherm constant are calculated from the graph of Freundlich adsorption isotherm.

$$\log q_e = \log K_f + \frac{1}{n} \log C_e \quad \text{Equation 2.4}$$

Where:

- C_e = Concentration after equilibrium (mg/L)
- q_e = Amount of metal adsorbed per gram of the adsorbent at equilibrium (mg/g)
- K_f = Freundlich isotherm constant (mg/g)
- $1/n$ = Slope of a graph

A function of the strength of adsorption process can be calculated from $1/n$ value. If n is equal to 1, the partition between the two phases are independent of the concentration. If $1/n$ value is below 1, it means a normal adsorption. If $1/n$ value is more than 1, it means cooperative adsorption. The cooperative adsorption refers to the interaction between adsorbent and adsorbate or between adsorbates (Liu, 2015).

Brunauer-Emmett-Teller (BET) Model is an extension of the Langmuir equation, which considers the multilayer adsorption. The BET model explains the physical adsorption of interaction between gas molecules and solid adsorption, which is applied to calculate pore size, average pore volume, and specific surface area.

Dubinin-Radushkevich equation is modified from Freundlich adsorption isotherm and used to describe the adsorption mechanism with a micropore volume filling on the heterogeneous adsorbent surface. Dubinin-Radushkevich equation is also written as Equation 2.5

$$\ln q_e = \ln q_s - K_{ad} \epsilon^2 \quad \text{Equation 2.5}$$

$$E = \frac{1}{\sqrt{2B_D}} \quad \text{Equation 2.6}$$

$$\epsilon = RT \ln \left(1 + \frac{1}{C_e} \right) \quad \text{Equation 2.7}$$

Where:

q_e = Amount of metal adsorbed (mg/g)

q_s = Theoretical isotherm saturation capacity (mg/g)

K_{ad} = Dubinin – Radushkevich isotherm constant (mol^2/kJ^2)

E = Energy of adsorption (kJ/mol)

B_D = Isotherm constant

ϵ = Dubinin – Radushkevich isotherm constant

R = Universal gas constant that is 8.314 J/mol/K

T = Temperature at 298 K

The energy of adsorption (E) value is shown adsorption mechanical on the adsorbent. If E value is lower than 8 kJ/mol, the adsorption mechanical is physical adsorption. If E value is between 8 – 16 kJ/mol, the adsorption mechanical is chemisorption.

2.2 Literature reviews

2.2.1 Reviews of diatomaceous earth

Inglethorpe et al. (1998) describes geology and depositional environment of diatomite in Lampang. Lampang Basin is a post-Oligocene intermontane basin. Diatomite was deposited under Quaternary fluvial gravels, sand and laterite in Ko Kha Formation of Mae Moh Group. As a result of Pleistocene tectonism, Neogene sediments were deposited while Lampang Basin was uplifted. Neogene sediments were produced by Quaternary river terrace and channel deposits. The silica enrichment of lake water is due to the devitrification of volcanic rocks that erupted in Pre-Neogene period. Kumanchan and Traiyan (1986) and Ratanasthien (1992) also found silica-rich in lake water and this silica is produced from air-fall ash at Mae Moh Basin. A study by Pariwatawon (1962) shows that Pliocene to recent freshwater diatoms species is the most abundant in Lampang Basin. Akutsu (1979) further identifies the species of diatoms to be *Melosira granulata*, *Navicula* and *Fragilaria*, are found in freshwater,

stagnant, eutrophic, and lacustrine depositional environment. Owen and Utha-aroon (1992) identifies another species of diatomite, that is *Aulacoseira*.

Mineralogy and petrography of diatomite Lampang, is described by Inglethorpe and Pearce (1999). From X-ray diffraction (XRD) results, diatomite is mainly composed of opal, clay mineral (smectite, kaolinite, and illite), quartz, and goethite. The diatomites from Lampang are classified into 3 types. First, diatomite that is mainly composed of whole strand-like colonies diatoms and the matrix is diatom fragments (Figure 2.2). The second type is laminae of diatoms with iron-stained and potassium rich clay mineral (Figure 2.3). The third type is mainly composed of diatom fragments with potassium rich clay matrix (Figure 2.4). In addition, Inglethorpe and Pearce (1999) are studied Cation Exchange Capacity (CEC) value of all types of diatomite. The cations such as Na^+ , Ca^{2+} , Mg^{2+} , and K^+ can exchange with heavy metals. The cation exchange capacity (CEC) of clayey diatomite (low quality) is 20.5 – 27.9 cmol/kg, which is higher than the diatomaceous type (high quality) that is 14.1 – 16.0 cmol/kg. Therefore, the clayey diatomite has a more effective removal than diatomaceous type.

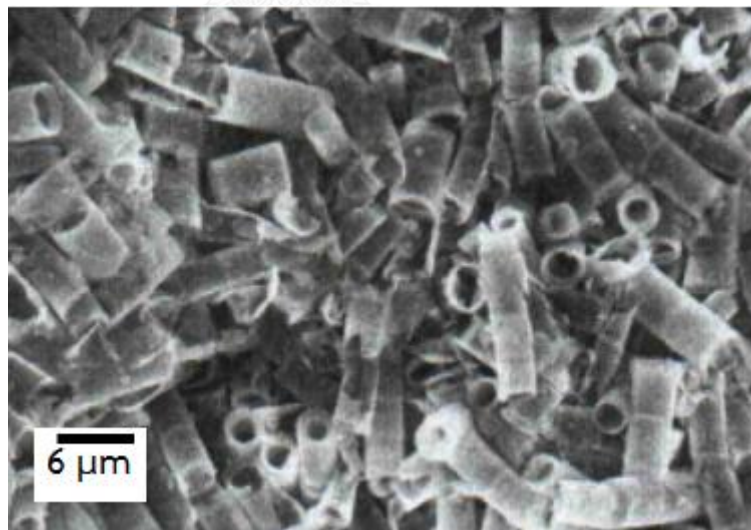


Figure 2.2 : A scanning Electron Microscopy (SEM) image of diatomite type 1 (after Inglethorpe and Pearce, 1999).

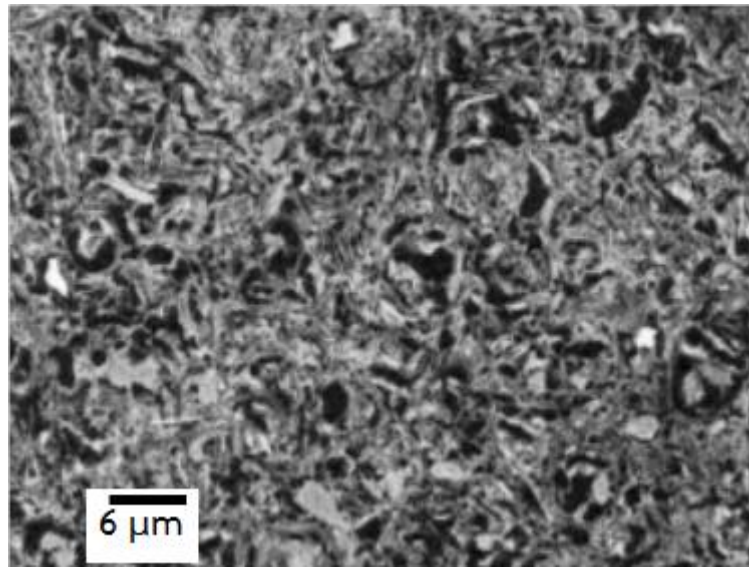


Figure 2.3 : A SEM image of diatomite type 2 (after Inglethorpe and Pearce, 1999).

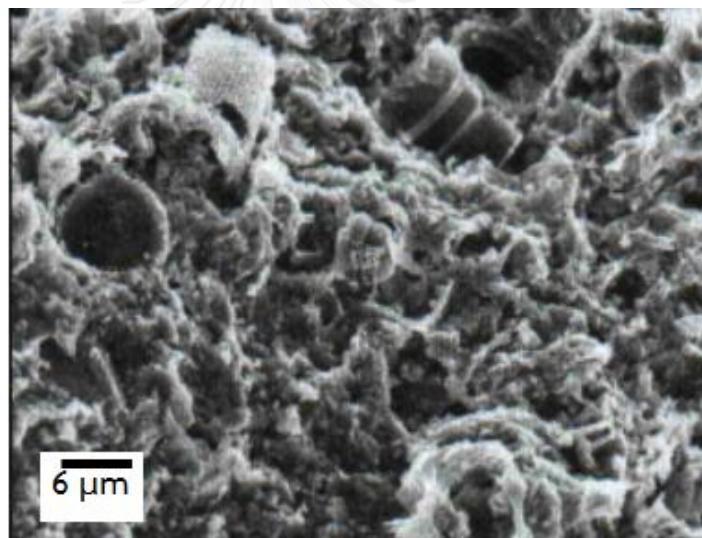


Figure 2.4 : A SEM image of diatomite type 3 (after Inglethorpe and Pearce, 1999).

Additionally, Inglethorpe et al. (1999) further investigated arsenic adsorbents made from diatomite from Lampang. Diatomites mainly contain opal, which is inert, rigid substrate for arsenic adsorption. Diatomite with iron-stained is used to treat As(V) contaminated water. The adsorption mechanism is physical adsorption. The behavior should be a monolayer adsorption for As(V). Langmuir Adsorption Isotherm is used to determine the maximum adsorption capacity for As(V) is 0.23 mg/g.

Diatomite has low density, low conductivity coefficient, weak adsorption capacity, but high porous structure. It contains mainly 87 – 91% of SiO₂, Al₂O₃ and

Fe_2O_3 . Several studies by Tsai et al. (2005); Tsai et al. (2004); Tsai et al. (2006) therefore, try to modify structure of diatomite using sodium hydroxide (NaOH) and hydrofluoric acid (HF) to improve its adsorbent capacity. The porosity and surface areas of diatomite is increased after adding 2.5N of HF for 1 hour at 60°C .

A study by Wu et al. (2005) uses iron hydroxide to coat diatomite for improving ability of arsenic adsorption. Modified diatomite by iron hydroxide has the maximum adsorption capacity of 61 mg/g in pH 7 and 17 mg/g in pH 2, whereas regular diatomite has the maximum adsorption capacity of only 1.98 mg/g in pH7. The initial arsenic concentration is 100 mg/l, the adsorbents are adsorbed 60 mg/l. Phosphate is an important anion that can interrupt the adsorption that adsorption effective could be decreased upto 50 percent.



2.2.2 Reviews of perlite and expanded perlite

Another geomaterial commonly used to make adsorbent is perlite. Cheungyuesuk and Suriyachai (1987) shows that perlite is mainly distributed in Lamnarai igneous complex in Lopburi and Petchabun. Saisutthichai (2006) informs that the only perlite mining company in Thailand is Klong Yang Company Limited. Perlite is commonly used as an adsorbent in fruit juice industry, soilless and hydroponic culture, and soil adjustment. Perlite is a glassy rhyolite and mainly composed of plagioclase, alkali feldspar, biotite and cristobalite. It has high surface area, high porous structure, lightweight and low density. Gunning (1994) suggests that a suitable density of perlite for an adsorption purpose is 112-192 kg/m^3 .

Alkan and Dogan (2001) uses H_2SO_4 modified perlite and expanded perlite for adsorbed Cu^{2+} . The Cu^{2+} removal percentage increases, when the pH of adsorbate increases. The Cu^{2+} removal percentage decreases, when ion strength and temperature increase. Chakir et al. (2002) investigates expanded perlite and bentonite to remove Cr^{3+} . The Cr^{3+} removal percentage increases, when the pH of adsorbate increases too. Expanded perlite can remove 40% of Cr^{3+} , and bentonite can remove 96% of Cr^{3+} .

Meesuk and Seammai (2010) modifies perlite structure by refluxing with 20% sodium hydroxide (NaOH) and 10% sulfuric acid (H_2SO_4) for 3 and 5 hours, to make an

adsorbent for dark-colored palm oil. Acid treated perlite cannot adsorb the dark-colored palm oil, but base treated perlite can. From X-ray diffraction (XRD), base treated perlite change the structure from amorphous to crystalline and namely zeolite Linde Type A and hydroxysodalite (Figure 2.5), which has high adsorption ability. According to X-ray fluorescence (XRF) analysis, perlite mainly composed of SiO_2 (75.2 wt %) and Al_2O_3 (12.8 wt %), which is suitable for making adsorbent and adsorbent. Cation exchange capacity (CEC) of base treated perlite is 20 – 33 cmol/kg. BET method is used to determine the surface area ($0.7891 \text{ m}^2/\text{g}$), pore size ($0.0068 \text{ cm}^2/\text{g}$), and pore volume (454 \AA). The results suggest that perlite has low cation exchange capacity although it has high porosity.

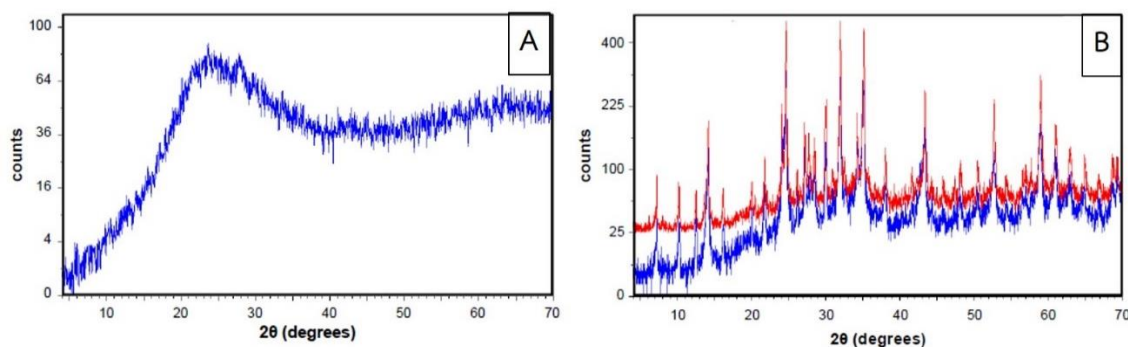


Figure 2.5 A XRD diffractogram of (A) non-treated expanded perlite and (B) base treated perlite. Red spectrum is 3 hours reflux and blue spectrum is 5 hours reflux (Meesuk and Seammai, 2010).

2.2.3 Reviews of other geological material

Branislava et al. (2011) compares properties of the others geological material such as zeolite, bentonite, sepiolite, limonite, pyrolusite, waste iron slag and water adsorbent sand. They are used to adsorb the As(III) and As(V) and analyzed the adsorption by Inductively coupled plasma mass spectrometry (ICP-MS). Concentrations of As(III) and As(V) are 0.5 mg/L. The contact time is 24 hours. Specific surface areas measured by BET method of all material are $45.5 \text{ m}^2/\text{g}$ for zeolite, $593.0 \text{ m}^2/\text{g}$ for bentonite, $286.0 \text{ m}^2/\text{g}$ for sepiolite, $1.7 \text{ m}^2/\text{g}$ for limonite, $1.2 \text{ m}^2/\text{g}$ for pyrolusite, $94.1 \text{ m}^2/\text{g}$ for waste iron slag and $2.9 \text{ m}^2/\text{g}$ for water adsorbent sand. Langmuir model is used to calculate the maximum adsorption capacity of zeolite is 0.97 mg/g for As(III) and 4.07 mg/g for As(V). The waste iron slag has the maximum adsorption capacity of 0.82 mg/g for As(III) and 4.04 mg/g for As(V). The water adsorbent sand has the

maximum adsorption capacity of 0.41 mg/g for As(III) and 0.77 mg/g for As(V). On the other hand, bentonite, pyrolusite and sepiolite are very affinity about arsenic adsorption.

Jiang et al. (2013) investigates arsenic contaminated groundwater and treatment options in Bangladesh. Important factors that affect the type of As in contaminated water are pH and redox potential. As (III) or arsenite is found as H_3AsO_3 , H_2AsO_3^- , and HAsO_3^{2-} , and stable at reduction condition. These compounds can react with iron and manganese hydroxides. On the other hand, As (V) or arsenate, are normally formed as H_3AsO_4 and AsO_4^{3-} at very low pH or high alkali condition, and found as H_2AsO_4^- at low pH, and form in HAsO_4^{2-} at high pH. There are 3 common treatment methods suggested. The first method involves co-precipitation, coagulation, and filtration processes, which can remove the arsenic about 90%. The composition of adsorbent includes activated alumina (Mn-coated and Fe-coated sand) and hydrated ferric oxide (HFO). HFO can adsorb As (III) and As (V), whereas activated alumina can only remove As(III). The second method involves precipitation and filtration at household scale. This method can remove the arsenic more than 90%, by adding ferric hydroxide and hypochlorite salt in the pumping wells. The last method is called base technique, which can remove arsenic more than 95%. The base technique uses iron-drop activated carbon, activated alumina, layered double hydroxide, and modified zeolites and clay to adsorb contaminated arsenic.

CHAPTER III

METHODOLOGY

This chapter discusses about geological material used to create the adsorbent and methods used to test the physical and chemical properties of the adsorbents. The adsorbents are tested in various conditions, i.e. pH, concentrations, contact time, the amount of adsorbents to find the most suitable condition for treating As contaminants. In addition, the adsorbents are tested with synthetic contaminated water and naturally contaminated groundwater samples.

3.1 Adsorbent preparations

The adsorbents used in this study are composed of three main components: siltstone, soil sample, and expanded perlite (Figure 3.1). Siltstone was collected from a roadcut outcrop (UTM : 554616E 2023114N) near Surasakmontri Hospital in Amphoe Mueang Lampang. Siltstone from this area is generally pale brown to brown and opaque and initially thought to be diatomite or diatomaceous earth due to its low density. However, laboratory analyses in this study cannot identify any diatom in the sample. The sample is thus called siltstone. Soil sample is very fine-grained and its fresh color is white. Expanded perlite was obtained from Klong Yang Mining in Amphoe Sa-Bot, Lopburi. Perlite is green and its weathering color is pale gray. After heating, perlite turns into white with volume expansion of 5 – 20 times. Siltstone, soil sample, and expanded perlite are grounded down to 100 mesh (0.149 mm.). All the geological materials are cleaned with deionized water for several times and dry at room temperature. After that, each geological material is analyzed employing X-ray diffraction (XRD) and X-ray fluorescence (XRF), respectively to identify its mineral and element compositions. Siltstone, soil sample, and expanded perlite powders are mixed with Mixture Design 3 compositions, which is the statistics computer program to determine proportions of adsorbent mixture. Adsorbents are heated at 700°C for 3 hours. Finally, all types of the adsorbents are tested for stability in deionized water. The surface area of the adsorbent is observed under Scanning Electron Microscope (SEM). The specific surface area, the pore size distribution and porous volume of a sample are calculated by using Brunauer, Emmett and Teller (BET) Theory.



Figure 3.1 : Geomaterials used to make the adsorbents. (A) siltstone, (B) soil sample, and (C) expanded perlite.

3.1.1 X-ray Diffraction (XRD)

Mineral compositions of all geological material are determined using X-ray Diffraction (XRD) at Department of Geology, Chulalongkorn University. Copper anode, which has a wavelength of 1.5418 \AA , is used to produce electrons to dislodge inner shell electrons of the target material. The X-rays are irradiated onto the sample at the angles from 5° to 70° . The intensity of the diffracted X-rays is recorded as shown in Figure 3.2. Bragg's Law (Equation 3.1) is used to calculate d-spacing values, and identify minerals based on their specific d-spacings.

$$n\lambda = 2d\sin\Theta \quad \text{Equation 3.1}$$

Where:

λ = X-ray wavelength (0.154nm)

Θ = A diffraction angle

d = A space between the lattice planes

n = positive integer

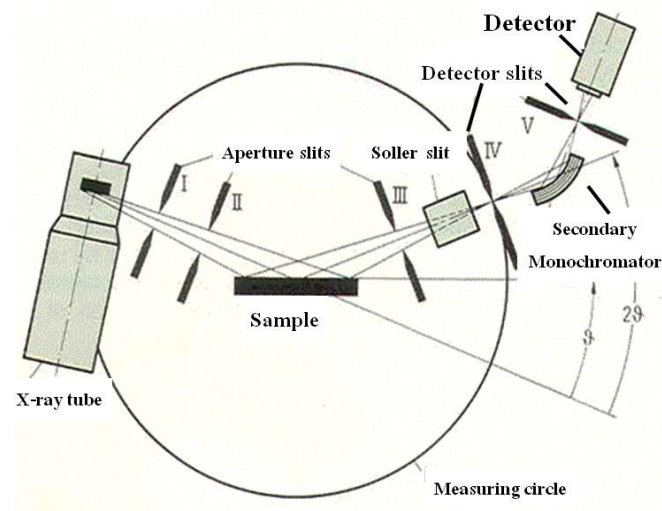


Figure 3.2 : A diagram of X-ray Diffraction method (after Silukkapatti, 2014).

3.1.2 Wavelength Dispersive X-ray Fluorescence (WDXRF)

Chemical compositions of geological material are determined by Wavelength Dispersive X-ray Fluorescence (WDXRF) at Department of Geology, Chulalongkorn University. When an atom absorbs high x-ray energy, it becomes excited and emits secondary X-rays. Each oxide compound emits X-rays at a unique energy. X-ray energy and characteristic of the emitted X-rays are measured the quantitative of each elements (Figure 3.3).

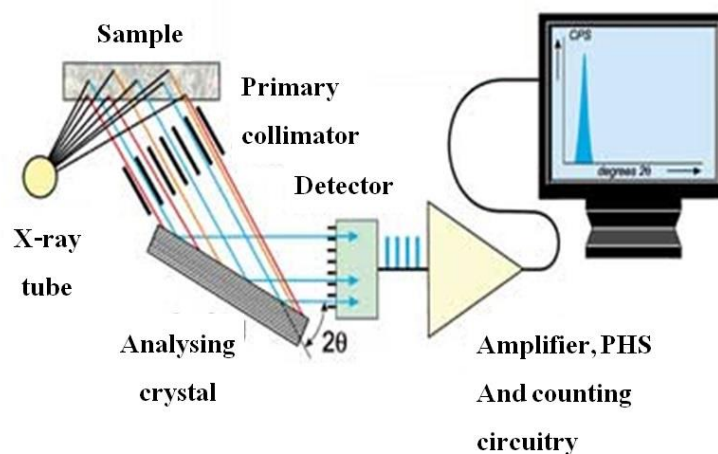


Figure 3.3 : A diagram of the operating system of X-Ray Fluorescence (after Wolska and Vrebos, 2004).

3.1.3 Mix and mold the adsorbents

Mixture Design is an experiment planner, which is based on the summary of all components is 1.0 or 100% and shown by trilinear coordinate system. The maximum and minimum values of each component are 100% and 0%, respectively. The amount of mixture type is calculated by Equation 3.2.

$$N = \frac{[(p + m) - 1]!}{[m!(p - 1)!]} \quad \text{Equation 3.2}$$

Where:

N = The amount of mixture type

m = Degree of division

p = Component

The program is called Minitab, used to suggest a design for adsorbents 3 components of degree of division is 3. The mixture is made up of 0, 1/3, 2/3, to 1. It suggested three points which are coordinated (2/3, 1/6, 1/6), (1/6, 2/3, 1/6), and (1/6, 1/6, 2/3) (Figure 3.4), which is whole comprehensive cases. In this study, the ratios of each adsorbent type are shown in Table 3.1.

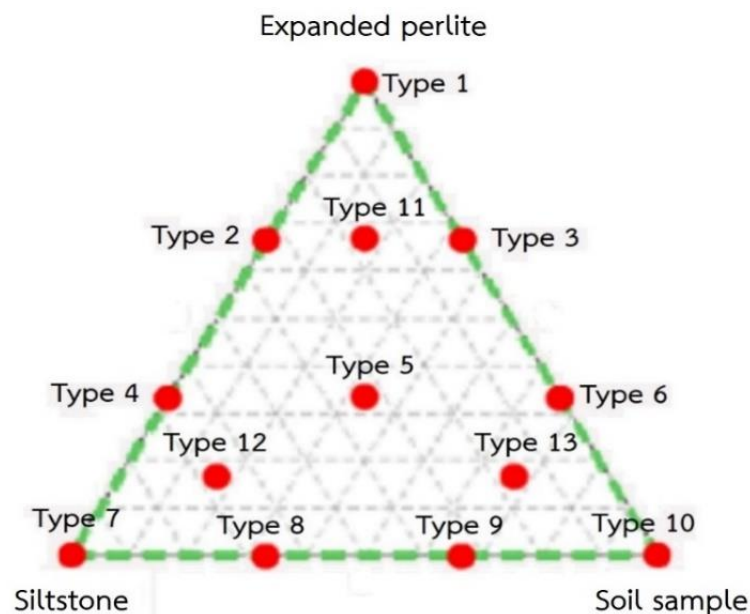


Figure 3.4 : A trilinear coordinate system from Minitab suggesting mixture design of adsorbents 3 components of degree 3 (Department of Statistics Online Programs, 2017).

Table 3.1 : Mixture Design of 3 components (by weight percent).

Type	Expanded perlite	Siltstone	Soil sample
1	100	0	0
2	66.67	33.33	0
3	66.67	0	33.33
4	33.33	66.67	0
5	33.33	33.33	33.33
6	33.33	0	66.67
7	0	100	0
8	0	66.67	33.33
9	0	33.33	66.67
10	0	0	100
11	66.67	16.67	16.67
12	16.67	66.67	16.67
13	16.67	16.67	66.67

3.1.4 Pore and surface of adsorbents

The specific surface area, the pore size distribution and porous volume of an adsorbent are studied by using Brunauer, Emmett and Teller (BET) Theory. The specific surface is related to the total surface area, which can be measured by the amount of adsorbed nitrogen gas. Based on BET theory, the nitrogen gas is adsorbed to a monomolecular layer on the adsorbent surface by Van der Waals forces. The specific surface area and porous volume are tested by BET method at Department of Science Service, Ministry of Science and Technology.

The porosity of samples before and after burning are observed using Scanning Electron Microscope (SEM) which is a high-resolution microscope using a tungsten tube to produce electrons. SEM has two detectors. The first one is a secondary electron detector used to observe the surface of the sample. The second one is backscattering-

electron detector used to measure the quantitative information about the sample composition (Figure 3.4). The surface of adsorbents is polished until smooth and studied by the SEM at Scientific and Technological Research Equipment, Chulalongkorn University.

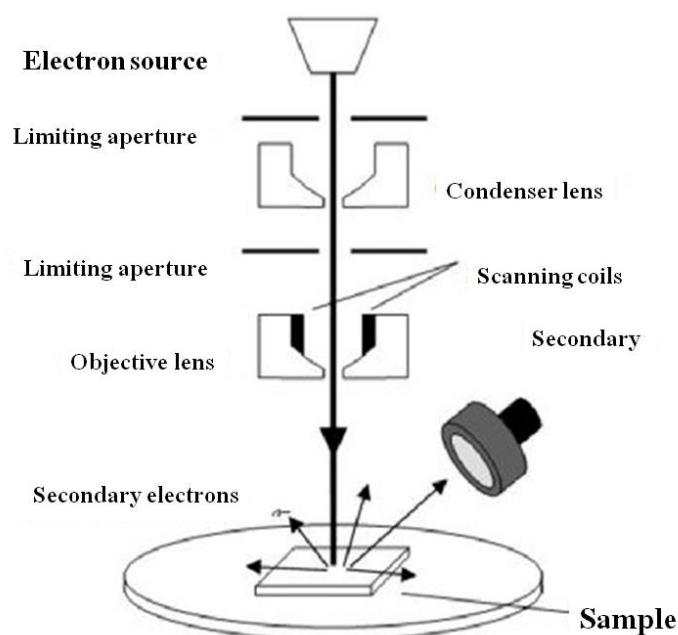


Figure 3.5 : A diagram of the operating system of SEM (after Department of Physics Warwick University, 2010).

จุฬาลงกรณ์มหาวิทยาลัย
CHULALONGKORN UNIVERSITY

3.1.5 Cation exchange capacity (CEC)

Cation exchange capacity (CEC) is a property of mineral that has negatively charged on its surface, which can adsorb the positively charged ions by electrostatic force. The main exchangeable cations are calcium (Ca^{2+}), magnesium (Mg^{2+}), sodium (Na^+) and potassium (K^+) (Rayment and Higginson, 1992). The cation exchange capacity (CEC) is tested at Department of Land Development, Ministry of Agriculture and Cooperatives.

3.2. Adsorption capacity test

The experiment is planned to study the As removal percentage in laboratory. The As contaminated water is prepared by diluted As(III) standard solution 1000 ppm (mg/L) with 1% HNO₃. The varying conditions in this experiment include the amount of adsorbents, the contact time, the initial concentration, and pH of the As contaminated water. In the first scenario which involves varying amount of adsorbents, the amounts adsorbent are 0.5, 1, 2.5, 5, 10, and 25 g for testing with 50 mL of water, 50 ppb of initial As concentration, and 60 minutes of contact time. In the second scenario, the contact times are varied from 15, 30, 45, 60, 90, 120, 150, and 180 minutes in tests that keep water volume (50 mL) and initial As concentration (50 ppb) constant and uses 10 g of adsorbent. In the third scenario, the initial As concentrations are varied from 5, 10, 20, 50, and 100 ppb in tests which keep water volume (50 mL), amount of adsorbent (10 g), and contact time (60 minutes) constant. The fourth scenario involves varying the pH value of As contaminated water by adjusting the pH by adding 1:1 HCl and 1:1 NaOH. The pH value are varied from 3, 5, 7, and 9 while keeping other parameters constant e.g. water volume (50 mL), initial As concentration (50 ppb), adsorbents (10 g), and the contact time (60 minutes).

Blank solution method is further used to compare the results of treatment. Blank solution is the dilute solution that has the same condition as the sample such as contact time, pH, amount of adsorbents, but it does not have the As contamination. In this experiment, the blank solution is 1% HNO₃.

As natural groundwater generally has a pH value of 7, more scenarios are tested when the pH of the solution to 7. As(III) is diluted to be a standard solution of concentration 1000 ppm with deionized water and adjusted the pH value with 1:1 HCl and 1:1 NaOH. The fifth scenario uses different pH values from 1, 4, 7, and 10 with 100 ppb of initial As concentration, 10 g of adsorbents, and 120 minutes of contact time. In the sixth scenario, the contact times are varied from 30, 60, 120, and 180 minutes in tests that keep water volume (50 mL) and initial As concentration (20 and 100 ppb) and uses 10 g of adsorbent. In the seventh scenario, the initial As concentrations are

varied from 20, 40, 60, 80, 100, 120, 140, 160, 180, and 200 ppb in tests which keep water volume (50 mL), amount of adsorbent (10 g), and contact time (120 minutes). In this experiment, the blank solution is deionized water (Table 3.2).

Table 3.2 : A summary of conditions used in adsorption capacity test.

Scenario	Diluent solution	Adsorbent (g.) / solution 50 ml.	Contact time (min)	Initial As concentration ($\mu\text{g/l}$)	pH
1	1% HNO_3	0.5, 1, 2.5, 5, 10, and 25	60	50	1.51
2	1% HNO_3	1	15, 30, 45, 60, 90, 120, 150, and 180	50	1.51
3	1% HNO_3	1	60	5, 10, 20, 50, and 100	1.51
4	1% HNO_3	1	60	50	3, 5, 7, and 9
5	Deionized water	10	120	100	1, 4, 7, and 10
6	Deionized water	10	30, 60, 120, and 180	20 and 100	7
7	Deionized water	10	120	20, 40, 60, 80, 100, 120, 140, 160, 180, and 200	7

Batch experiment is used to mix between adsorbents and As contaminated water. Solution was shaken at 180 round per minute (rpm) at room temperature. After that, the solution was filtered with filter paper for separate adsorbents and the

solution. The solution was measured for As removal using Graphite-Furnace Atomic Absorption Spectroscopy (GFAAS) and calculated the As removal percentage by Equation 3.3.

$$\% \text{Removal} = \frac{(C_0 - C_e) \times 100}{C_0} \quad \text{Equation 3.3}$$

Where:

C_0 = Concentration in the initial solution

C_e = Concentration after equilibrium

Graphite-Furnace Atomic Absorption Spectroscopy (GFAAS) is the equipment, which analyzed the trace elements in the sample. GFAAS uses the graphite furnace to vaporize the liquid sample. Free atoms can absorb specific light frequencies or wavelengths of the element. Concentration measurements are determined from the standard calibration curve. This equipment is suitable for analyzing trace and ultra-trace elements. The detection limit of the GFAAS for total As is 2 ppb.

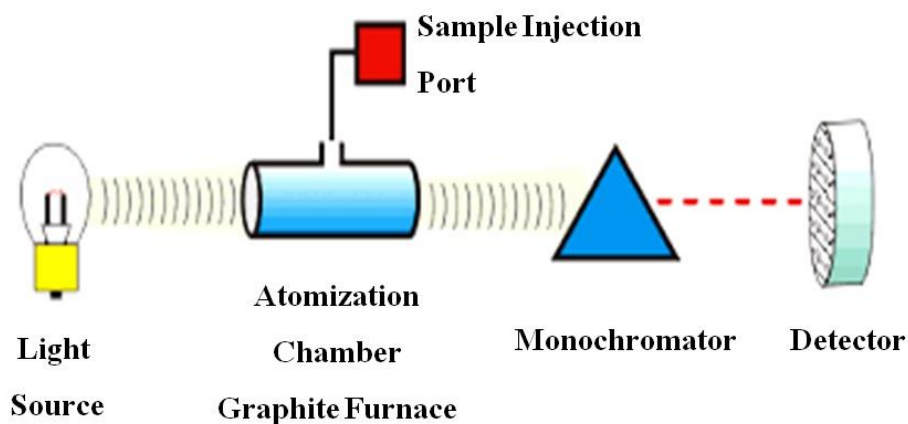


Figure 3.6 : A diagram of Graphite Furnace Atomic Absorption Spectroscopy (GFAAS) (after Verma, 2014).

3.3 Adsorbent testing in Natural Contaminated Groundwater

Groundwater samples were collected from Amphoe Dan Chang in Suphan Buri and Amphoe Ban Rai in Utthai-Thani. Groundwater samples were collected in 2 polyethylene bottles. Then, 5 ml of 1:1 HNO₃ acid was added in 1 bottle for preserving the natural condition. The value of pH, conductivity, salinity, and total dissolved solids (TDS) were measured by a multipurposed pH meter. The initial As concentrations of groundwater samples were determined by GFAAS. Each 50 mL of groundwater sample was treated with 10 g of adsorbents, remeasured for the remaining As concentration, and calculated for the As removal percentage.

Inductively Coupled Plasma Optical Emission Spectrometry (ICP-OES) was used to determine other initial cation concentrations of groundwater. ICP-OES uses the plasma to vaporize the liquid sample, then photon of the cation is emitted the specific spectrum (Figure 3.7). Concentration measurements are determined from the standard calibration curve. This equipment is suitable for analyzing multiple elements. The remaining others cation concentration in groundwater samples is determined again by ICP-OES.

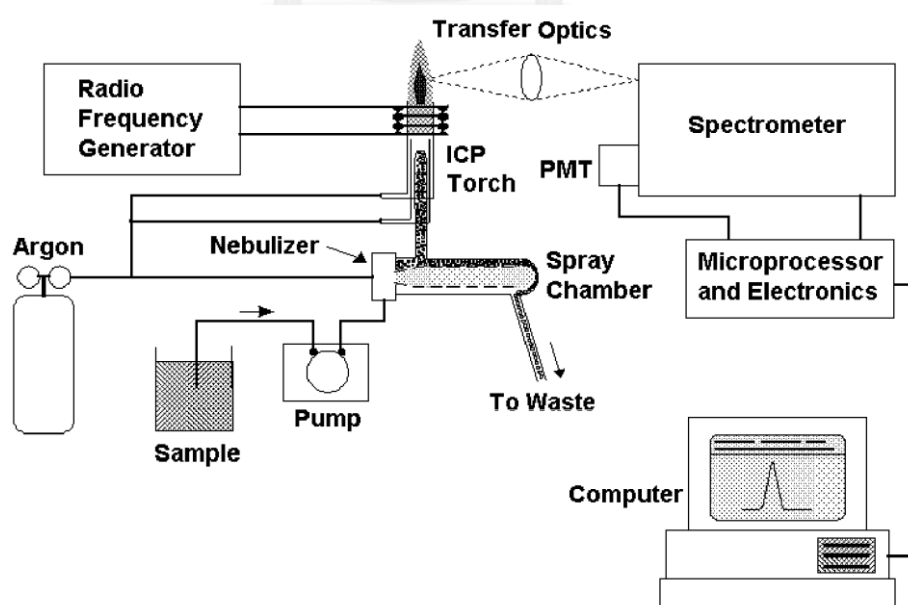


Figure 3.7 : A diagram of Inductively Coupled Plasma Optical Emission Spectrometry (ICP-OES) (after Boss and Fredeen, 2004).

The concentrations of fluoride (F⁻) and chloride (Cl⁻) were determined by ion selective electrode. Phosphate (PO₄³⁻) was determined by spectrophotometer, which is determine the transmission of the solution as a wavelength. Phosphate reacts with ammonium molybdate under acidic condition by adding HNO₃. The phosphate-contaminated groundwater is changed from colorless to yellow in 30 minutes.



CHAPTER IV

RESULTS

This chapter summaries results of experiments and laboratory works, including chemical composition of adsorbents analyzed by XRD and XRF, porosity and surface area by BET method, and the efficiency of As adsorption measured by GFAAS and CEC.

4.1 Adsorbents preparation

4.1.1 Composition of geomaterials

4.1.1.1 Siltstone

Siltstone was collected from Amphoe Mueang Lampang, which is pale brown, dull luster, and opaque. Specific gravity is approximately 1.97. Results from XRD show that it is mainly composed of quartz (blue), goethite (red), illite (green), opal-CT (orange), and kaolinite (purple) as shown in Figure 4.1. From the XRD pattern, 2θ angles is range of 19 to 24 is shown the amorphous structure, and 2θ angle is approximately 21.729, it shows the peak of opal (cristobalite and tridymite). XRF results confirm that siltstone has SiO_2 (69.40%), Al_2O_3 (18.90%) and Fe_2O_3 (5.05%) as major components. While others oxides are found less than 5% (Table 4.1). The siltstone sample has a similar properties like diatomite, but from SEM image (Figure 4.2), it cannot find any diatoms that should be namely siltstone.

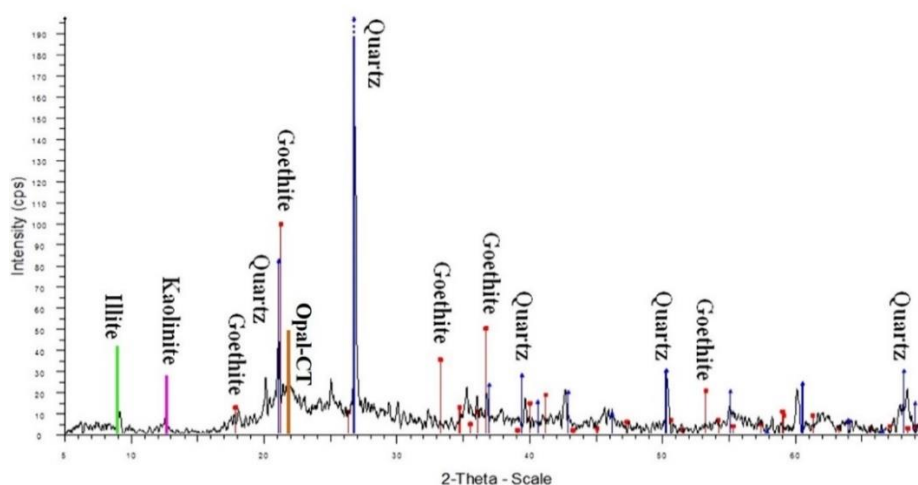


Figure 4.1 : A X-ray diffraction pattern of siltstone.

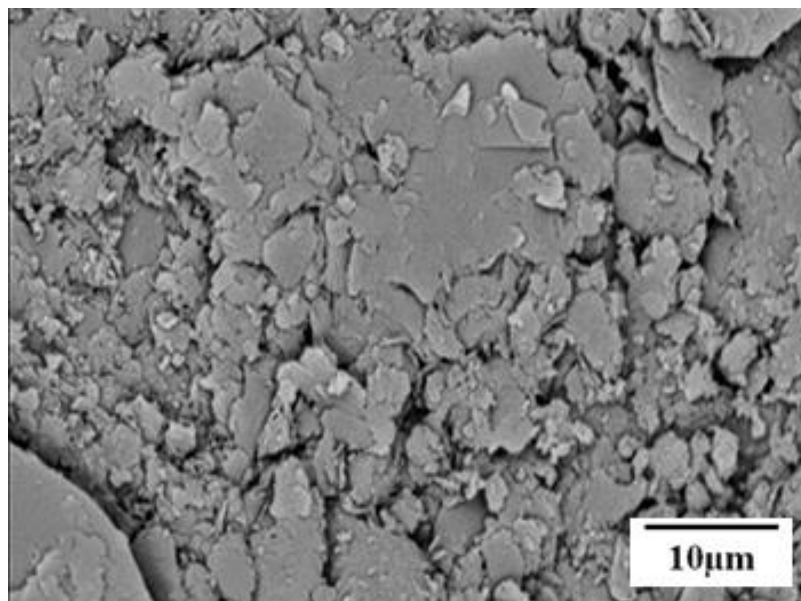


Figure 4.2 : A SEM image of siltstone.

Table 4.1 : The oxide composition of siltstone (weight percent) analyzed by XRF.

Chemical composition	Siltstone (wt %)
SiO ₂	67.4
Al ₂ O ₃	16.9
Fe ₂ O ₃	4.05
K ₂ O	2.89
SO ₃	1.11
MgO	0.89
TiO ₂	0.82
Na ₂ O	0.4
CaO	0.23
LOI	5.29
Total	99.98

4.1.1.2 Expanded perlite

Expanded perlite was obtained from Klong Yang Mining in Amphoe Sa-Bot, Lopburi, which is light weight, white, dull luster, and opaque. Expanded perlite is more porous structure and more adsorption efficient than natural perlite. Results from XRD show that expanded perlite consists of amorphous quartz and aluminium oxide (Figure 4.3). XRF results confirm that expanded perlite has SiO_2 (74.10%), Al_2O_3 (13.50%) and K_2O (7.30%) as major components. While others oxides are found less than 5% (Table 4.2).

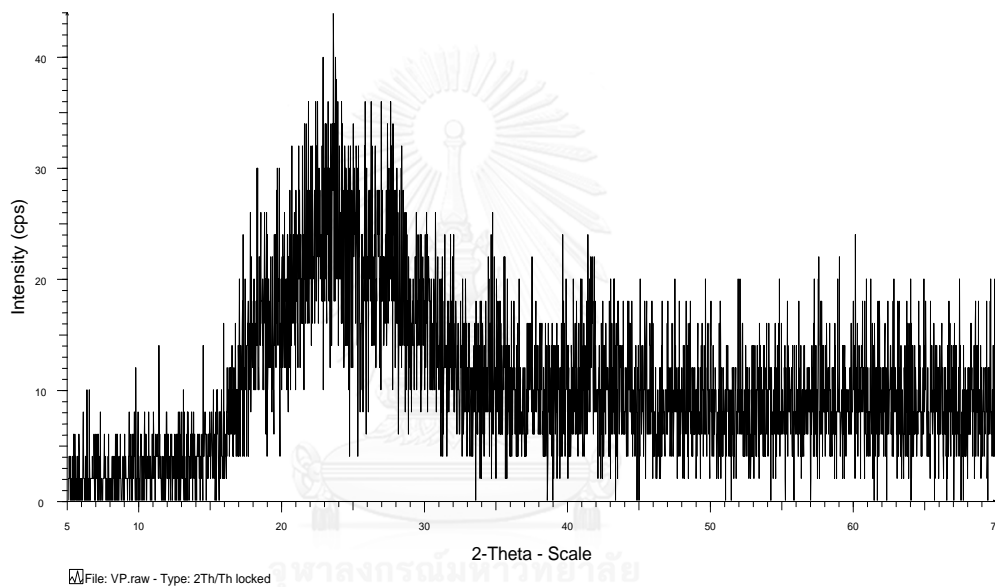


Figure 4.3: A X-ray diffraction pattern of expanded perlite.

Table 4.2 : The oxide composition of expanded perlite (weight percent) analyzed by XRF.

Chemical composition	Expanded perlite (wt %)
SiO ₂	72.1
Al ₂ O ₃	13.5
Fe ₂ O ₃	1.66
K ₂ O	7.3
MgO	0.23
TiO ₂	0.29
Na ₂ O	1.59
CaO	1
LOI	2.30
Total	99.97

4.1.1.3 Soil sample

This study soil sample was obtained from Lampang Kaolin Mining Company Limited in Amphoe Chae Hom, Lampang, which is white, dull luster, and opaque. Results from XRD show that it is composed of quartz (red), kaolinite (green) and illite (blue) as shown in Figure 4.4. XRF results confirm that soil sample has SiO₂ (80.60%), Al₂O₃ (14.60%) and K₂O (3.48%) as major components. While others oxides are found less than 5% (Table 4.3).

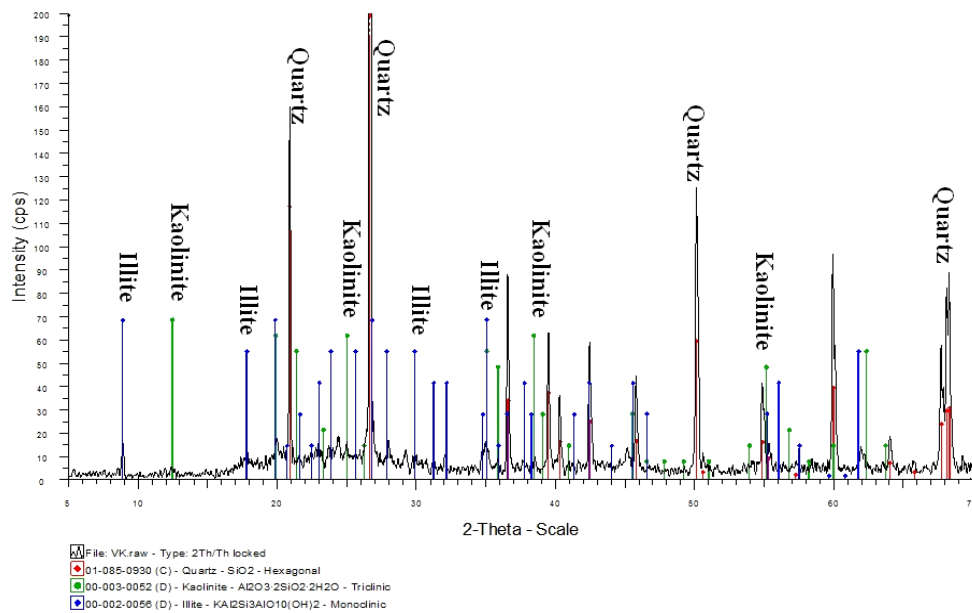


Figure 4.4 : A X-ray diffraction pattern of soil sample.

Table 4.3 : The oxide composition of soil sample (weight percent) analyzed by XRF.

Chemical composition	Soil sample (wt %)
SiO ₂	80.60
Al ₂ O ₃	14.60
Fe ₂ O ₃	0.46
K ₂ O	3.48
MgO	0.11
Na ₂ O	0.34
CaO	0.07
LOI	0.27
Total	99.93

4.1.2 Mold adsorbent

Each geomaterial (siltstone, expanded perlite and soil sample) is mixed in different ratios in order to find the most stable adsorbent for arsenic removal. Adsorbent type 1 is composed of expanded perlite (100 wt%) and has white color. Type 1 adsorbent is not very stable after drying (Figure 4.5).



Figure 4.5 : The adsorbent type 1.

Adsorbent type 2 is composed of expanded perlite (66.67 wt%) and siltstone (33.33 wt%) and has pale brown color. Type 2 adsorbent remains intact after drying (Figure 4.6).



Figure 4.6 : The adsorbent type 2.

Adsorbent type 3 is composed of expanded perlite (66.67 wt%) and soil sample (33.33 wt%) and has white color. Type 3 adsorbent partially disintegrates and collapses after drying (Figure 4.7).



Figure 4.7 : The adsorbent type 3.

Adsorbent type 4 is composed of expanded perlite (33.33 wt%) and siltstone (66.67 wt%) and has brown color. Type 4 adsorbent completely disintegrates and collapses after drying (Figure 4.8).



Figure 4.8 : The adsorbent type 4.

Adsorbent type 5 is composed of expanded perlite (33.33 wt%), siltstone (33.33 wt%), and soil sample (33.33 wt%) and has pale brown color. Type 5 adsorbent remains intact after drying (Figure 4.9).



Figure 4.9 : The adsorbent type 5.

Adsorbent type 6 is composed of expanded perlite (33.33 wt%) and soil sample (66.67 wt%) and has white color. Type 6 adsorbent partially disintegrates and collapses after drying (Figure 4.10).



Figure 4.10 : The adsorbent type 6.

Adsorbent type 7 is composed of siltstone (100 wt%) and has brown color. Type 7 adsorbent completely disintegrates and collapses after drying (Figure 4.11).



Figure 4.11 : The adsorbent type 7.

Adsorbent type 8 is composed of siltstone (66.67 wt%) and soil sample (33.33 wt%) and has brown color. Type 8 adsorbent partially disintegrates and collapses after drying (Figure 4.12).



Figure 4.12 : The adsorbent type 8.

Adsorbent type 9 is composed of siltstone (33.33 wt%) and soil sample (66.67 wt%) and has brown color. Type 9 adsorbent remains intact after drying (Figure 4.13).



Figure 4.13 : The adsorbent type 9.

Adsorbent type 10 is composed of soil sample (100 wt%) and has white color. Type 10 adsorbent remains intact after drying (Figure 4.14).



Figure 4.14 : The adsorbent type 10.

Adsorbent type 11 is composed of expanded perlite (66.67 wt%), siltstone (16.67 wt%), and soil sample (16.67 wt%) and has white color. Type 11 adsorbent is not very stable after drying (Figure 4.15).



Figure 4.15 : The adsorbent type 11.

Adsorbent type 12 is composed of expanded perlite (16.67 wt%), siltstone (66.67 wt%), and soil sample (16.67 wt%) and has brown color. Type 12 adsorbent remains intact after drying (Figure 4.16).



Figure 4.16 : The adsorbent type 12.

Adsorbent type 13 is composed of expanded perlite (16.67 wt%), siltstone (16.67 wt%), and soil sample (66.67 wt%) and has brown color. Type 13 adsorbent remains intact after drying (Figure 4.17).



Figure 4.17 : The adsorbent type 13.

In summary, adsorbents type 2, 5, 9, 10, 12 and 13 remain consolidated after drying. Adsorbent type 12 (siltstone : expanded perlite : soil sample = 0.6667 : 0.1667 : 0.1667) is the most stable adsorbent, because it was easy to mold and the shape of the

adsorbent is very well intact In contrast, adsorbent type 7 (siltstone : expanded perlite : soil sample = 1 : 0 : 0) completely disintegrates and collapses after drying. The adsorbent types which mainly contain of expanded perlite such as types 1 and 11, they are not very stable after drying.

After heating adsorbents at 700°C for 3 hours, and submerging them in deionized water, most types of adsorbents, except for type 12, become unconsolidation. Each type breaks down at varying contact time. Type 5 takes the least amount of time within 2 minutes to disaggregate. Type 2, 9, 10, and 13 break down in 3 – 15 minutes. Type 12 is the only adsorbent that remains intact after days and the most suitable candidate to test for As removal (Figure 4.18).

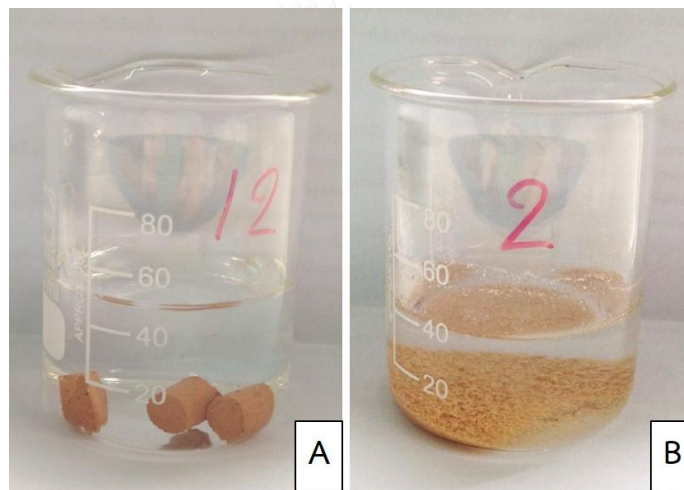


Figure 4.18: A dissolution of the adsorbents after puts in the water. Adsorbent type 12 (A) being still constant, and Adsorbent type 2 (B) is the representation of the tender types.

Results from XRD show that the adsorbent type 12 is mainly composed of quartz (red), muscovite (blue), illite (purple) and kaolinite (green) as shown in Figure 4.19. XRF results confirm that the adsorbent type 12 has SiO_2 (69.12%), Al_2O_3 (15.01%), Fe_2O_3 (2.57%), and K_2O (3.52%) as major components. While others oxides are found less than 5% (Table 4.4).

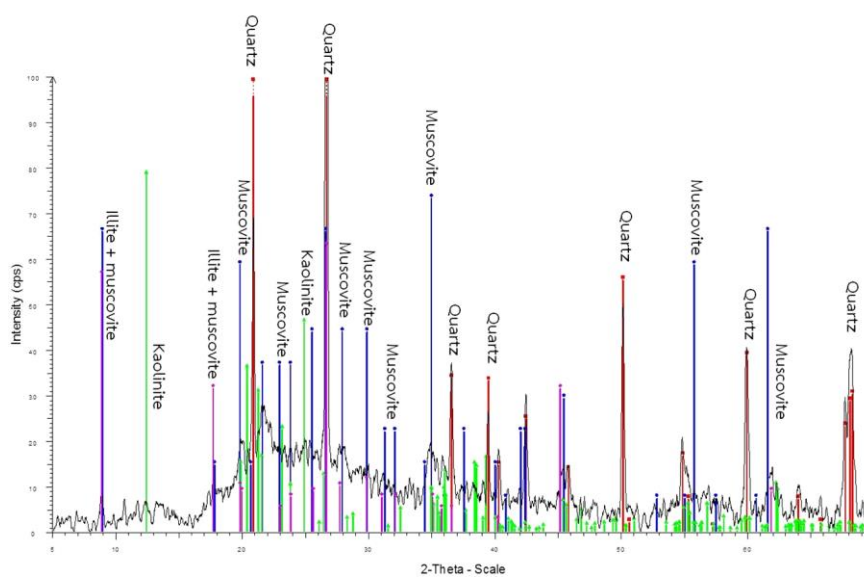


Figure 4.19 : A X-ray diffraction pattern of adsorbent type 12.

Table 4.4 : The oxide composition of adsorbent type 12 (weight percent) analyzed by XRF.

Chemical composition	Adsorbent type 12 (wt %)
SiO ₂	69.12
Al ₂ O ₃	15.01
Fe ₂ O ₃	2.57
K ₂ O	3.52
Na ₂ O	0.75
MgO	0.52
TiO ₂	0.42
CaO	0.49
SO ₃	0.62
LOI ⁻	6.60
Total	99.61

MAUD software is used to measure the quantitative of adsorbents type 12. Mineral composition of adsorbents type 12 is mainly composed of silica – alumina glass (86.69 wt%), quartz (6.48 wt%), Illite – mica (2.04 wt%), kaolinite (1.87 wt%), muscovite (1.48%), illite (1.05 wt%), and montmorillonite (0.40 wt%) (Figure 4.20).

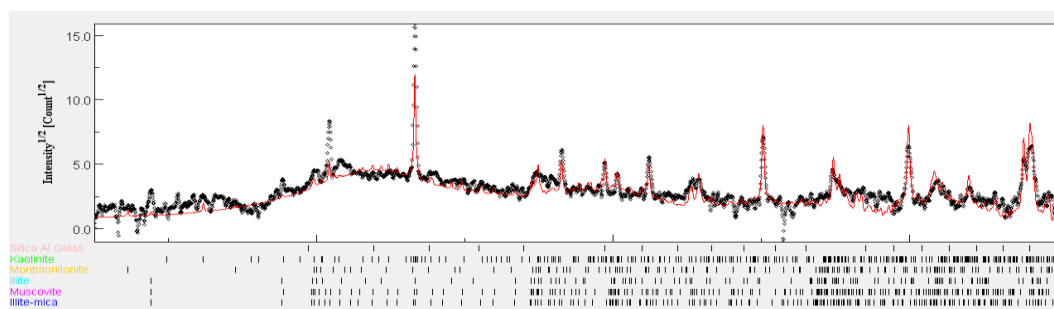


Figure 4.20 : A X-ray diffraction pattern of adsorbent type 12.

4.1.3 Porosity and Microstructures

Results from BET measurements show that the specific surface area of unheated adsorbent type 12 is $28.2 \text{ m}^2/\text{g}$, the pore volume is $0.097 \text{ cm}^3/\text{g}$, and the average pore size is 137.2 \AA (mesopore range). The specific surface area of heated adsorbent type 12 is $32.6 \text{ m}^2/\text{g}$, the pore volume is $0.099 \text{ cm}^3/\text{g}$, and the average pore size is 121.4 \AA (mesopore range). The specific surface area and pore volume of heated adsorbent type 12 were increased. However, pore size of heated adsorbent type 12 was decreased. The SEM images of the porous structure, unheated and heated adsorbent are shown in Figure 4.21 and 4.22. The microstructure surfaces of adsorbents are different in size and shape, suggesting that the surface of the adsorbent is heterogeneous.

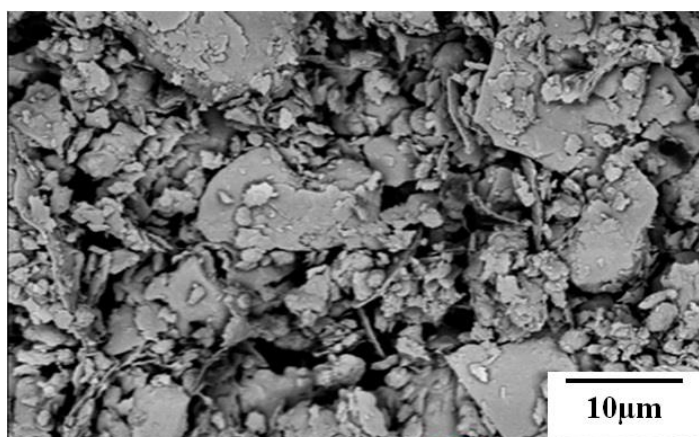


Figure 4.21 : A SEM image of porous structure of the unheated adsorbent.

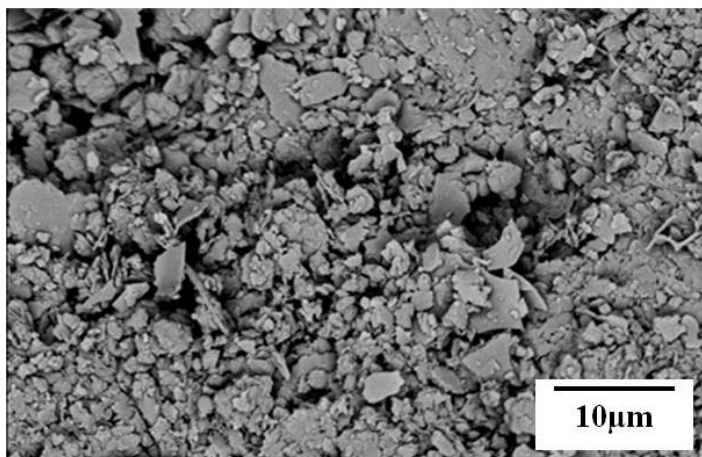


Figure 4.22: A SEM image of small porous structure of the heated adsorbent.

4.1.4 Cation exchange capacity (CEC)

The cation exchange capacity (CEC) is the value of the ability that is the reaction between the ion of the adsorbent surface and the solution. The CEC of adsorbent type 12 is 10.94 cmol/kg. The CEC of raw material, that are siltstone (2.07 cmol/kg), soil sample (4.91 cmol/kg.), and expanded perlite (20.14 cmol/kg.).

4.2 Adsorption efficiency

4.2.1 Scenario 1 : effect of adsorbent dose

As(III) removal percentage increases as a function of the amount of adsorbent when adding more amount of the adsorbent, from 0 to 4.78, 48.55, 75.1, 91.38 and more than 99.99 % (Table 4.5). However, the percentage of arsenic removal is almost saturated when the adsorbent is approximate 10 grams for 50 ml of water as shown in Figure 4.23. The highest arsenic removal efficiency was almost 100% in the amount of adsorbent was 25g. By varying the amount of adsorbent, the more adsorbent added the more removal percentage observed. The result of variation of amount of adsorbent was shown in Appendix A, Table A1.

Table 4.5 : The variation of adsorbent amount.

Amount sample (g.)	C_0 (ppb)	C_e (ppb)	% As removal
0.5	50	44.52	11.05
1	50	33.64	32.76
2.5	50	25.86	47.30
5	50	21.50	57.47
10	50	4.83	90.37
25	50	0.20	99.59

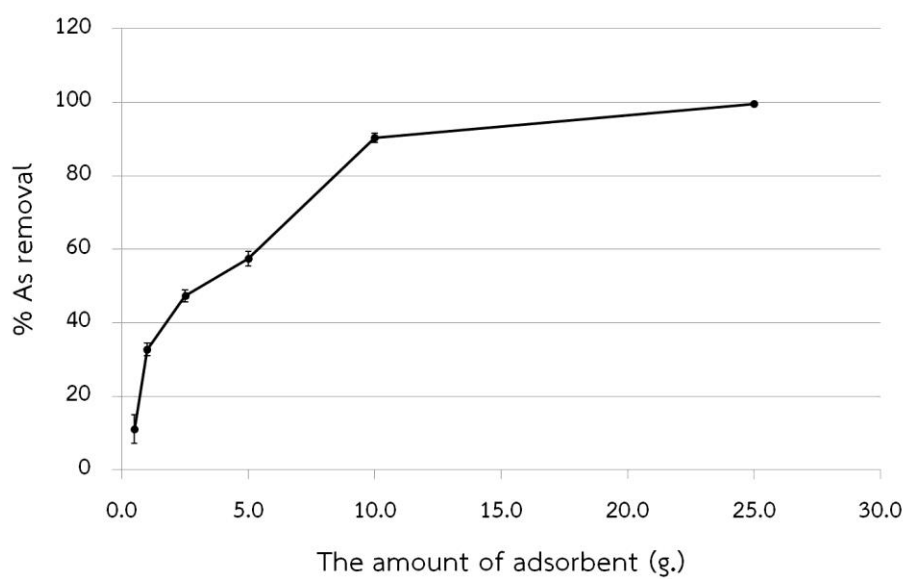


Figure 4.23 : Arsenic removal percentage as a function of the amount of the adsorbent added.

4.2.2 Scenario 2 : effect of contact time

The As(III) removal percentage increases as a function of the contact time, from 4.94 to 10.88, 13.1, 25.7, 39.64 and 97.40 % (Table 4.6). The arsenic removal efficiency was zero to 4.95% at the contact time was 0 to 15 minutes. After contacting water more than 2 hours, the adsorption ability becomes saturated as shown by a steady removal percentage of As, which is 97.40% (Figure 4.24). The result of variation of contact time was shown in Appendix A, Table A2.

Table 4.6: The variation of contact time.

Contact time (min)	C_0 (ppb)	C_e (ppb)	% As removal
0	50	49.52	0.97
5	50	47.17	4.15
10	50	45.03	12.68
30	50	42.73	15.32
60	50	36.75	27.32
90	50	30.83	38.84
120	50	1.42	97.13
150	50	1.14	97.76
180	50	0.83	98.32

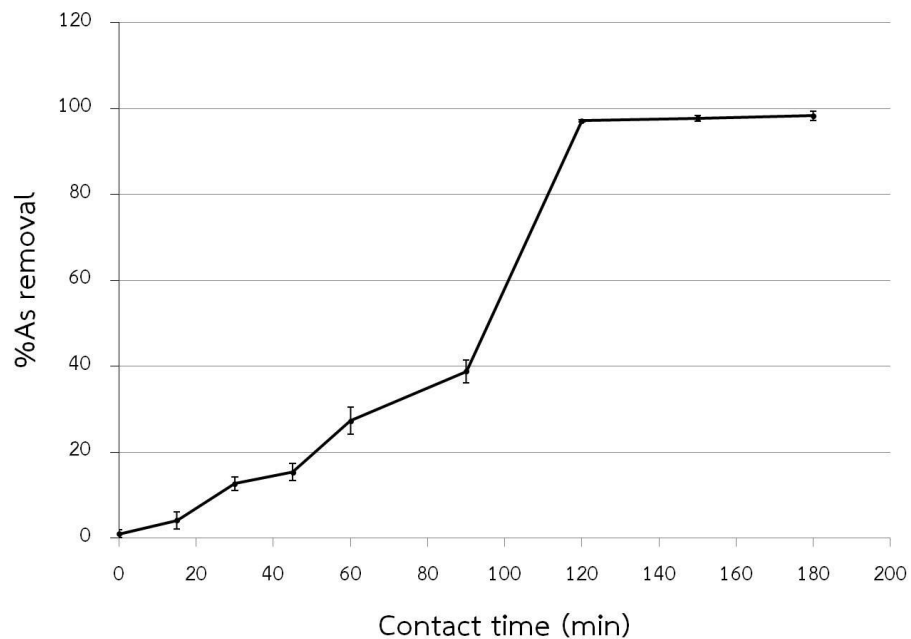


Figure 4.24 : Arsenic removal percentage as a function of the contact time.

4.2.3 Scenario 3 : effect of concentration of As

The As(III) removal percentage decreases as a function of the arsenic concentration, when using the higher concentration. The initial concentration (C_0) of As(III) is varied from 10 to 100 ppb, and the others condition has remained constant. The As(III) removal percentage is 70.80 % for the initial As concentration is 10 ppb, 46.40 % for the initial As concentration is 20 ppb, 34.64 % for the initial As concentration is 50 ppb, and 5.90 % for the initial As concentration is 100 ppb as shown in Table 4.7 and Figure 4.25. The result of variation of concentration was shown in Appendix A, Table A3.

Table 4.7 : The variation of concentration (C_0).

C_0 (ppb)	C_e (ppb)	% As removal
5	0.34	94.39
10	2.62	74.03
20	10.68	47.97
50	32.70	34.12
100	92.67	7.68

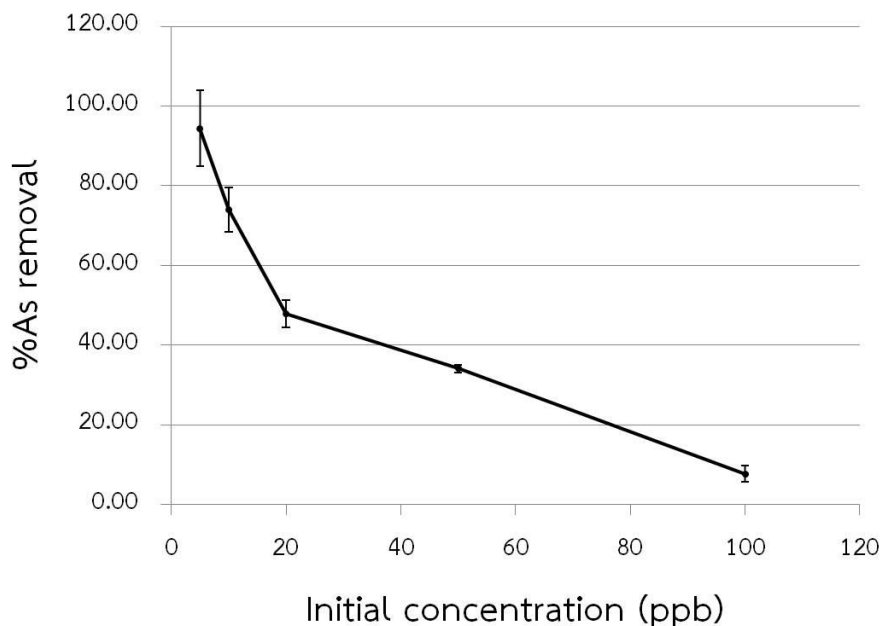


Figure 4.25 : Arsenic removal percentage as a function of the concentration.

4.2.4 Scenario 4 : effect of pH

The As(III) removal percentage increases as a function of the pH of the As contaminated water, when the pH value is higher, from 44.67 to 47.57 and 48.60%. However, when the pH value is 9 the arsenic removal percentage decreases to 46.78%. The initial pH of As contaminated water is 7, that has the highest percentage of arsenic removal. Moreover, after adsorption, the pH value of the tested water was dropped. This means that the adsorbent is acid material. From the study, the initial pH is 7 is the suitable condition for used the adsorbent (Table 4.8 and Figure 4.26). The result of variation of pH was shown in appendix A, Table A4.

Table 4.8 : The variation of pH for As concentration is 50 ppb.

pH		C_0 (ppb)	C_e (ppb)	% As removal
Before	After			
3	2.87	50	27.86	44.64
5	3.24	50	26.96	47.57
7	3.34	50	25.47	48.60
9	3.63	50	27.03	46.78

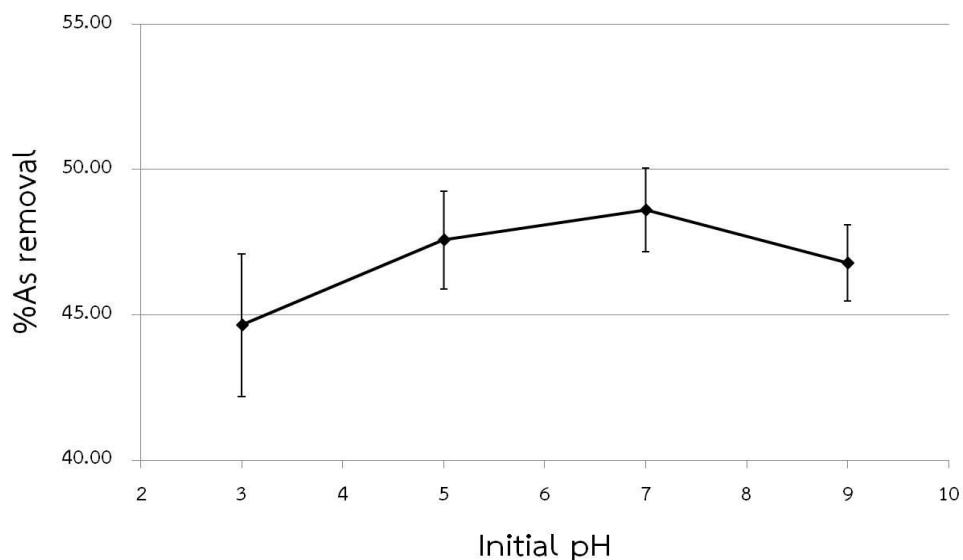


Figure 4.26 : Arsenic removal by varying pH value.

From the studies of the arsenic removal from standard solution of As (III), the suitable initial pH of the solution is 7, however the As removal percentage of each pH value is nearly by the others. After that, spread range of pH value and higher concentration are designed to study, which the initial pH is suitable for As(III) removal. According to the previous study, the amount of adsorbent is used in this thesis is 10 grams for the solution is 50 ml., the contact time is 2 hours.

4.2.5 Scenario 5: effect of pH (As concentration 50 ppb)

The arsenic removal percentage increases as a function of the pH, when the pH value is higher, from 6.81 to 28.16, 36.81% for the initial concentration of 100 ppb. However, when the pH value is 10 the arsenic removal percentage decreases to 33.13% as shown in Table 4.9. From the study of variable pH, arsenic can be best removed when the pH of solution is around 7 (Figure 4.27). The result of variation of pH was shown in Appendix A, Table A5.

Table 4.9 : The variation of pH for As concentration is 100 ppb.

pH		C ₀ (ppb)	C _e (ppb)	% As removal
Before	After			
1	2.12	100	93.33	6.82
4	3.98	100	72.60	28.16
7	5.25	100	63.25	36.81
10	9.23	100	67.36	33.13

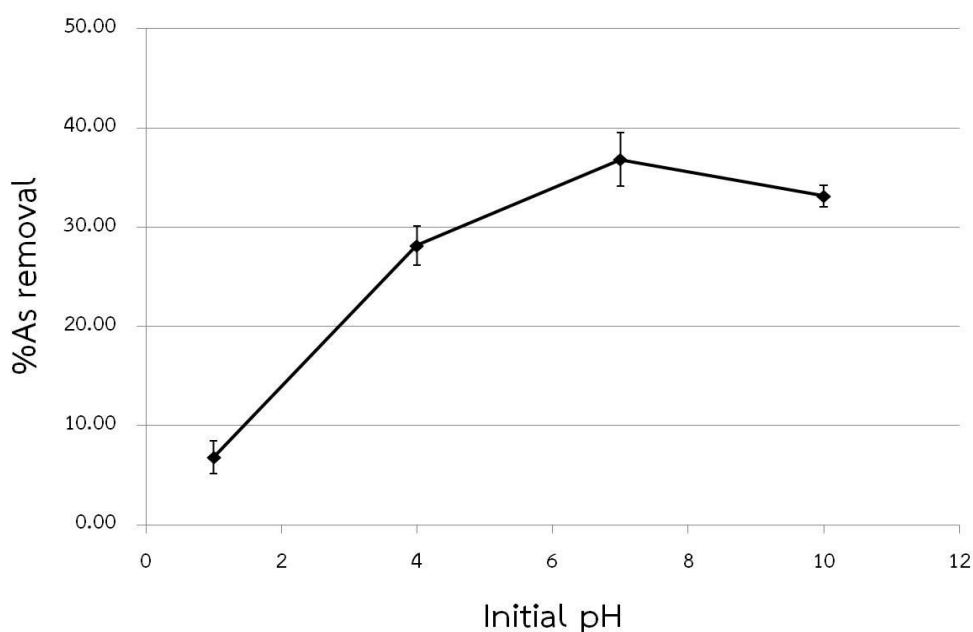


Figure 4.27 : Arsenic removal by varying pH value.

4.2.6 Scenario 6: effect of contact time after adjusting the pH contaminated water to 7

The arsenic removal percentage increases as a function of the contact time from 11.30 to 14.24 and 28.42% for the initial concentration is 20 ppb. However, when the contact time is 180 minutes, the arsenic removal percentage decreases to 16.52%. In addition, the arsenic removal percentage decreases when the contact time increases, from 20.78 to 17.05% for the initial concentration is 100 ppb, . The As removal percentage increases to 33.16% when contact time is 120 minute. However,

when the contact time is 180 minutes, the arsenic removal percentage decreases to 28.79% as shown in Table 4.10. The highest percentage of arsenic removal when the contact time is 2 hours. The arsenic removal percentage of the initial concentration is 100 ppb (upper line, Figure 4.28) is higher than the initial concentration is 20 ppb (lower line, Figure 4.28). For this study, the contact time, which suitable for As(III) removal with this adsorbents is 2 hours. The complete results of contact time variation are shown in Appendix A, Table A6.

Table 4.10 : The variation of contact time at pH equal to 7.

Contact time (min)	C ₀ (ppb)	C _e (ppb)	% As removal
30	20	18.07	11.30
60	20	17.32	14.24
120	20	14.83	28.42
180	20	16.82	16.52
30	100	78.62	20.78
60	100	83.23	17.05
120	100	66.19	33.16
180	100	71.31	28.79

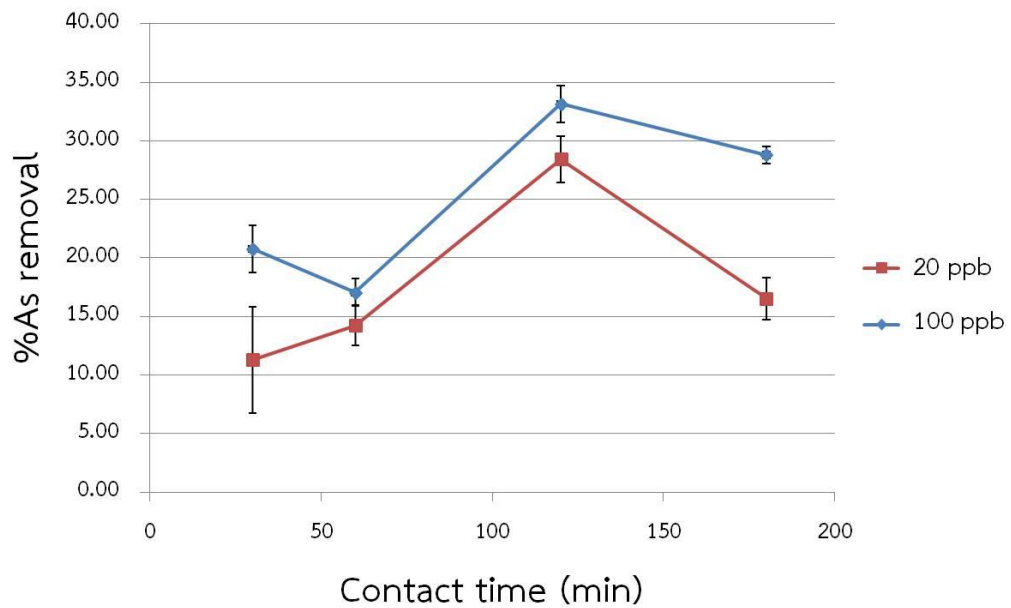


Figure 4.28 : Arsenic removal percentage as a function of the contact time.

4.2.7 Scenario 7 : effect of As concentration after adjusting the pH to 7

The arsenic removal percentage increases as a function of the initial concentration, from 37.92 to 38.50, 38.79, 39.45, and 41.39%. The As removal percentage trends to be constant, after the concentration is 100 ppb, the As removal percentage rises in slowly, and decreases as shown in Table 4.11 and Figure 4.29. This result is conflicted with the previous test, because of the initial pH of the As contaminated waters are different. The initial pH of the first As contaminated water is 1.52, but the initial pH of the second As contaminated water is adjusted to 7. The result of variation of concentration was shown in Appendix A, Table A7.

Table 4.11 : The variation of concentration at pH equal to 7.

C_0 (ppb)	C_e (ppb)	% As removal
20	12.15	37.92
40	25.54	38.50
60	36.32	38.79
80	46.36	39.45
100	60.34	41.39
120	65.24	45.88
140	69.56	50.08
160	70.46	56.31
180	71.64	60.77
200	74.55	63.00

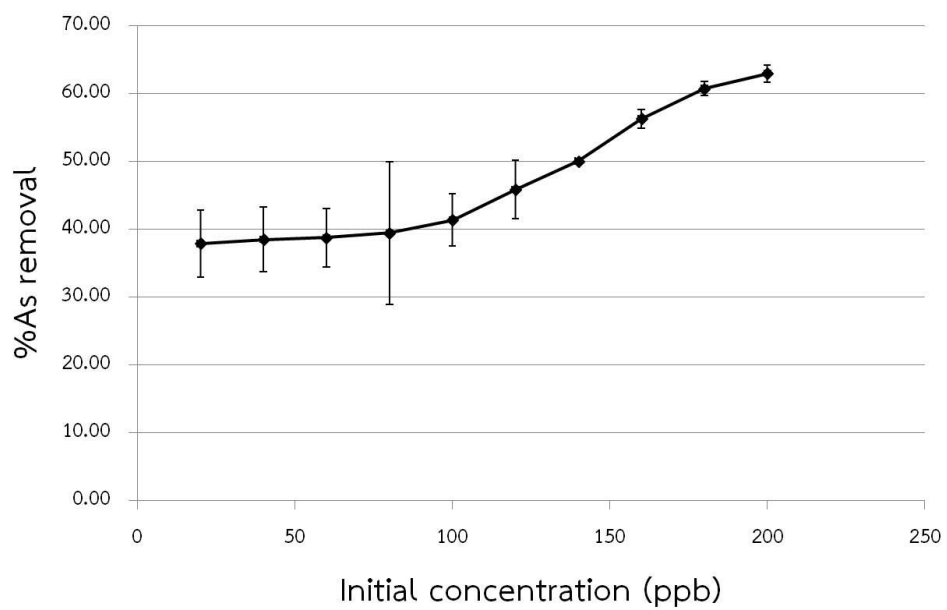


Figure 4.29 : Arsenic removal percentage as a function of the concentration.

4.3 Adsorbent testing in natural contaminated groundwater

Results of The sampling point and some properties of groundwater sample are shown in Table 4.12, and concentration of cation and anion contaminated in groundwater are shown in Table 4.13 and appendix A, Table A7. The As removal percentage of each sample was calculated as shown in Table 4.14 and appendix A, Table A8 and A9. The comparison of the initial As concentration and the remaining As concentration after treatment are shown in Figure 4.30.

Table 4.12 : The sampling point and some properties of groundwater sample.

Sample	UTM		pH	Conductivity (S/m)	Salinity (g/kg)	TDS (ppm)
	East	North				
GW01	574393	1662479	7.15	784	0.3	384
GW02	572070	1662765	6.95	676	0.4	332
GW03	574443	1660777	7.05	599	0.3	294
GW04	573698	1660345	7.25	931	0.5	456
GW05	573445	1660443	7.18	839	0.5	411
GW06	576177	1659953	7.03	128	0.1	261.2
GW07	576018	1659218	7.16	170	0.1	83
GW08	575934	1658647	7.01	95	0.1	47
GW09	571838	1657667	7.25	549	0.3	268
GW10	572695	1656286	7.35	640	0.3	314
GW11	573434	1647990	7.08	791	0.4	388

Table 4.13 : The concentrations of cation and anion in groundwater sample before and after treatment. Treated sample is in italic and marked with an asterisk sign (*).

Sample	As (ppb)	Ca (ppm)	Fe (ppm)	K (ppm)	Mg (ppm)	Na (ppm)	F ⁻ (ppm)	PO ₄ ³⁻ (ppm)	Cl ⁻ (ppm)	pH
GW01	139.33	28.67	0.04	3.94	19.38	132.63	1.07	22.56	109.33	7.15
<i>GW01*</i>	<i>99.67</i>	<i>71.02</i>	<i>0.04</i>	<i>41.48</i>	<i>30.99</i>	<i>154.05</i>	<i>0.84</i>	<i>18.61</i>	<i>107.33</i>	<i>6.09</i>
GW02	17.10	112.70	0.09	6.13	19.51	9.78	0.50	12.87	14.00	6.95
<i>GW02*</i>	<i>8.60</i>	<i>134.65</i>	<i>0.09</i>	<i>14.87</i>	<i>31.98</i>	<i>13.76</i>	<i>0.29</i>	<i>10.54</i>	<i>10.00</i>	<i>6.42</i>
GW03	26.24	67.75	0.38	2.69	23.70	19.97	0.70	12.86	29.00	7.05
<i>GW03*</i>	<i>9.39</i>	<i>108.56</i>	<i>0.40</i>	<i>10.75</i>	<i>39.53</i>	<i>25.87</i>	<i>0.20</i>	<i>10.32</i>	<i>25.00</i>	<i>6.32</i>
GW04	147.00	5.52	0.40	9.19	2.99	4.29	0.00	26.98	9.00	7.25
<i>GW04*</i>	<i>36.30</i>	<i>36.96</i>	<i>0.35</i>	<i>21.76</i>	<i>28.49</i>	<i>19.49</i>	<i>0.00</i>	<i>23.96</i>	<i>4.00</i>	<i>6.84</i>
GW05	42.67	28.94	0.22	2.65	28.44	38.45	0.90	15.51	52.00	7.18
<i>GW05*</i>	<i>32.00</i>	<i>70.60</i>	<i>0.04</i>	<i>39.10</i>	<i>37.44</i>	<i>63.72</i>	<i>0.63</i>	<i>10.74</i>	<i>33.33</i>	<i>6.26</i>
GW06	80.33	38.46	0.10	5.42	8.56	47.53	0.44	11.82	47.00	7.03
<i>GW06*</i>	<i>50.33</i>	<i>77.59</i>	<i>0.02</i>	<i>43.07</i>	<i>21.73</i>	<i>70.35</i>	<i>0.32</i>	<i>7.52</i>	<i>40.00</i>	<i>5.98</i>
GW07	38.70	17.37	21.68	7.97	8.94	54.06	0.60	26.87	25.00	7.16
<i>GW07*</i>	<i>15.20</i>	<i>35.97</i>	<i>18.34</i>	<i>44.21</i>	<i>18.74</i>	<i>77.36</i>	<i>0.20</i>	<i>15.26</i>	<i>21.00</i>	<i>6.74</i>
GW08	362.30	38.51	0.04	0.72	51.24	60.73	3.14	42.53	34.67	7.01
<i>GW08*</i>	<i>259.00</i>	<i>82.23</i>	<i>0.03</i>	<i>39.73</i>	<i>57.55</i>	<i>89.54</i>	<i>2.29</i>	<i>39.34</i>	<i>30.67</i>	<i>5.87</i>
GW09	39.67	64.32	0.05	0.59	22.21	60.41	0.27	21.91	114.67	7.25
<i>GW09*</i>	<i>31.67</i>	<i>113.87</i>	<i>0.02</i>	<i>41.20</i>	<i>34.20</i>	<i>92.20</i>	<i>0.25</i>	<i>18.94</i>	<i>103.33</i>	<i>7.01</i>
GW10	93.80	30.09	0.13	7.22	5.50	24.92	0.30	23.89	10.00	7.35
<i>GW10*</i>	<i>38.20</i>	<i>78.32</i>	<i>0.12</i>	<i>31.96</i>	<i>36.07</i>	<i>67.98</i>	<i>0.28</i>	<i>21.76</i>	<i>5.00</i>	<i>6.91</i>
GW11	16.13	112.70	0.09	6.13	19.51	9.78	0.50	17.43	14.00	7.08
<i>GW11*</i>	<i>8.08</i>	<i>216.54</i>	<i>0.08</i>	<i>18.65</i>	<i>48.07</i>	<i>41.76</i>	<i>0.46</i>	<i>15.55</i>	<i>11.00</i>	<i>6.37</i>

Table 4.14 : The percentages of arsenic removal in groundwater samples after treating with geo-adsorbents.

Sample	C ₀ (ppb)	C _e (ppb)	% Arsenic Removal
GW01	139.33	99.67	28.46
GW02	17.10	8.60	49.71
GW03	26.24	9.39	64.21
GW04	147.00	36.30	75.31
GW05	42.67	32.00	25.01
GW06	80.33	50.33	37.35
GW07	38.70	15.20	60.72
GW08	362.30	259.00	28.51
GW09	39.67	31.67	20.17
GW10	93.80	38.20	59.28
GW11	16.13	8.08	49.91

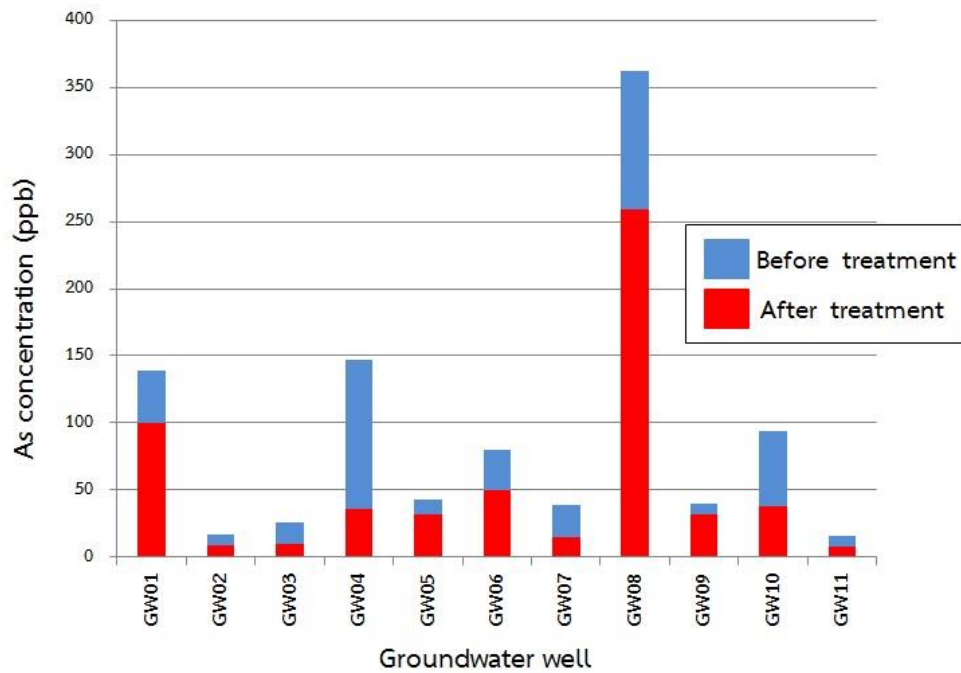


Figure 4.30 : The comparison of the initial As concentration and the remaining As concentration after treatment.

From the study, the adsorbent can adsorb arsenic fairly well. The As removal percentage are between 20.17% to 75.31 % for the initial As concentrations between 16.13 to 362.30 ppb.

CHAPTER V

DISCUSSION

This chapter discusses the adsorption mechanisms that occur in the treatment of As-contaminated water. The isotherms are used to describe the mechanism of adsorbents and the adsorption capacity. The properties of adsorbents in this study are compared to previously studied adsorbents such as specific surface area and cation exchange capacity.

In this study show that, expanded perlite is helping to mold, because it has a high surface tension. However, the composition of expanded perlite is too much, it yield the adsorbent is brittle. Soil sample was helped to combine between siltstone and expanded perlite.

5.1 The adsorption mechanism

The adsorption test performed to find suitable conditions for As treatment such as variation of pH, initial concentration, amount of adsorbent and contact time. Suitable conditions refer to the conditions at which adsorption, for this study is used 10 grams of adsorbents for the solution 50 ml in pH 7. The contact time is 2 hours. The adsorption mechanism is studied by varying initial concentration and plotted the graph of solid-liquid distribution coefficient. The amount of As adsorbed (q_e) was calculated by Equation 2.1 and shown in Table 5.1.

Table 5.1 : The As concentration of the initial solution (C_0) and the As concentration after equilibrium (C_e) and the amount of As adsorbed (q_e).

Initial As concentration; C_0 ($\mu\text{g/L}$)	As concentration after equilibrium; C_e ($\mu\text{g/L}$)	Amount of adsorped As; q_e (mg/g)
20	12.15	37.10
40	25.54	79.95
60	36.32	115.10
80	46.36	151.05
100	60.34	213.03
120	65.24	276.55
140	69.56	348.93
160	70.46	454.02
180	71.64	554.98
200	74.55	634.57

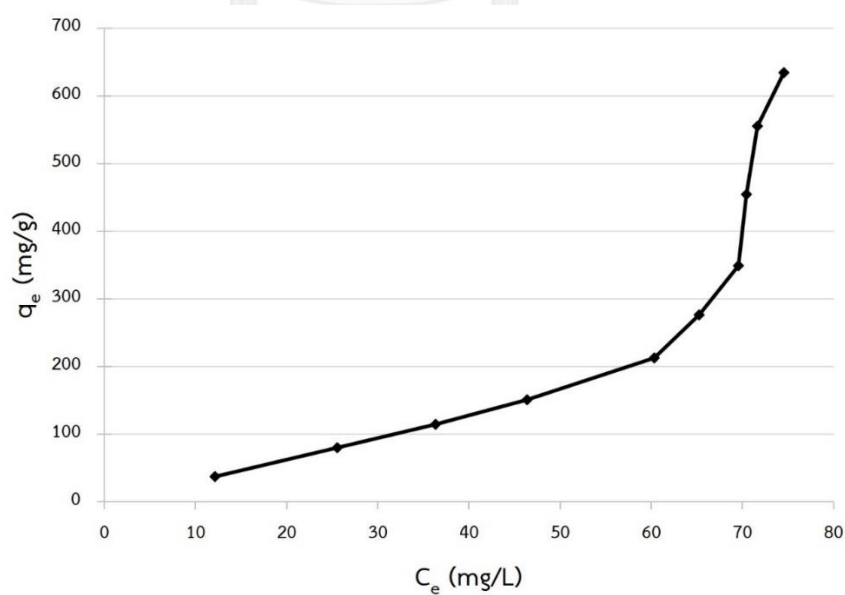


Figure 5.1: A graph of solid – liquid distribution coefficient.

The slope of the graph of solid-liquid distribution coefficient gradually increases at low As concentrations (10-60 mg/L) and exponentially rises at high As concentrations (60-80 mg/L) (Figure 5.1). According to Weber and Chakravorti (1974) (Figure 2.2), the shape of graph curve implies to unfavorable that means the interaction between adsorbents and adsorbate was reversible because of the adsorbate was desorbed from the adsorbents.

5.2 The Adsorption Isotherm

The adsorption isotherm models are used to describe the effect of arsenic concentration that adsorbed on the adsorbent surface. The adsorption isotherm models used in this study are Langmuir and Freundlich models. The Langmuir adsorption isotherm is used to describe the monolayer adsorption on the homogeneous surface. While the Freundlich adsorption isotherm is used to explain the multilayer adsorption on the heterogeneous surface.

5.2.1 Langmuir Adsorption Isotherm

Langmuir adsorption isotherm is the ideal of adsorption. It used to describes the mechanism adsorption, which the surface of adsorbent is a perfectly flat plain and homogeneous. The adsorbent can adsorb one element on to monolayer, and do not have interaction between adsorbate molecules. Langmuir adsorption isotherm is also written as Equation 2.2, and the maximum capacity and Langmuir isotherm constant are calculated from the graph of Langmuir adsorption isotherm (Figure 5.2). The mechanism of adsorption (R_L) is calculated by Equation 2.3.

R_L value is indicated the mechanism of adsorption. If R_L is more than 1, the mechanism of adsorption is unfavorable. If R_L is 1, the mechanism of adsorption is linear. If R_L is range from 0 to 1, the mechanism of adsorption is favorable. Moreover, if R_L is 0, the mechanism adsorption is irreversible.

Table 5.2 : Parameters used in Langmuir Adsorption Isotherm calculation

C_0 ($\mu\text{g/L}$)	C_e ($\mu\text{g/L}$)	q_e (mg/g)	$1/C_e$ (L/ μg)	$1/q_e$ (g/mg)	R_L
20	12.15	37.1	0.0823	0.02695	1.12
40	25.54	79.95	0.03915	0.01251	1.25
60	36.32	115.1	0.02753	0.00869	1.36
80	46.36	151.05	0.02157	0.00662	1.46
100	60.34	213.033	0.01657	0.00469	1.62
120	65.24	276.55	0.01533	0.00362	1.72
140	69.56	348.933	0.01438	0.00287	1.83
160	70.46	454.017	0.01419	0.0022	1.97
180	71.6433	554.983	0.01396	0.0018	2.09
200	74.5467	634.567	0.01341	0.00158	2.21

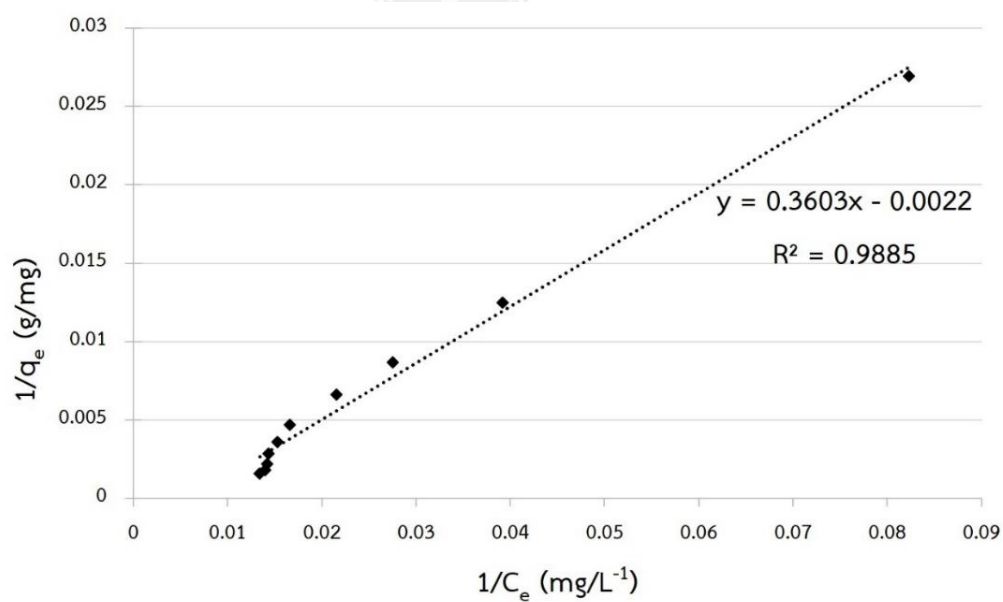


Figure 5.2 : A graph of Langmuir Adsorption Isotherm.

Table 5.3 : Results from Langmuir Adsorption Isotherm.

Constant	Value
$1/Q_0$	0.22
Q_0 (mg/g)	0.45
K_L (L/mg)	6.11
R_L	1.12 – 2.21
R^2	0.98

From the Figure 5.2 and Table 5.2 and 5.3, the slope of the graph ($1/Q_0$) is 0.22. The maximum capacity (Q_0) is 0.45 mg/g. The R^2 of Langmuir adsorption isotherm is 0.98. The R^2 value is the coefficient of determination. If R^2 is 0%, it cannot explain the variability of the response data. In other hand, if R^2 is 100%, it is suitable for explained the variability of the response data. In addition, the R_L values are 1.12 to 2.21 that means the adsorption is unfavorable.

5.2.2 Freundlich Adsorption Isotherm

Freundlich adsorption isotherm is used to describe the adsorption, where the surface of the adsorbent is heterogeneous. The adsorbent can adsorb more than one layer, and the adsorbate molecules are interact to the adsorbents (Equation 2.4).

$1/n$ value is a function of the strength of adsorption process. If $n=1$, it means the partition between the two phases are independent of the concentration. If $1/n$ value is below 1, it means a normal adsorption. If $1/n$ value is more than 1, it means cooperative adsorption.

Table 5.4 : Parameters used in Freundlich Adsorption Isotherm calculation.

C_0	C_e	q_e	$\log C_e$	$\log q_e$
20	12.15	37.1	1.08458	1.56937
40	25.54	79.95	1.40722	1.90282
60	36.32	115.1	1.56015	2.06108
80	46.36	151.05	1.66614	2.17912
100	60.3433	213.033	1.78063	2.32845
120	65.24	276.55	1.81451	2.44177
140	69.5633	348.933	1.84238	2.54274
160	70.4567	454.017	1.84792	2.65707
180	71.6433	554.983	1.85518	2.74428
200	74.5467	634.567	1.87243	2.80248

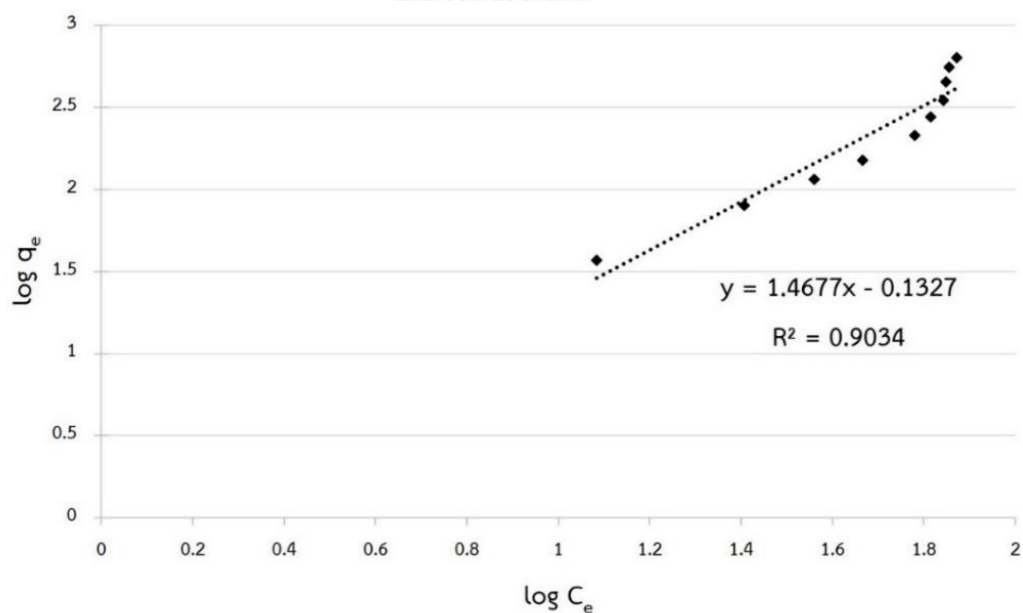


Figure 5.3 : A graph of Freundlich Adsorption Isotherm.

Table 5.5 : Results from Freundlich Adsorption Isotherm.

Constant	Value
1/n	1.27
n	0.79
K_f (mg/g)	1.47
R^2	0.90

From the Figure 5.3 and Table 5.4 and 5.5, the slope of the graph (1/n) is 1.27. The Freundlich isotherm constant (K_f), which referred to adsorption capacity is 1.47 mg/g. The R^2 of Freundlich adsorption isotherm is 0.90. Moreover, the 1/n value is more than 1, it means cooperative adsorption. Cooperative adsorption is described the adsorption mechanism is caused by interaction between solutions and/or between solution and adsorbent, which is multilayer adsorption.

5.2.3 The Dubinin – Radushkevich Adsorption Isotherm

Dubinin – Radushkevich adsorption isotherm is applied from Freundlich adsorption isotherm, which used to describe the adsorption mechanism with a pore-filling adsorption on the heterogeneous adsorbent surface. Moreover, the Dubinin - Radushkevich adsorption isotherm (Equation 2.5, 2.6 and 2.7) are used to plot the Dubinin – Radushkevich Adsorption Isotherm graph. The energy of adsorption (E) value is shown adsorption mechanical on the adsorbent. If E value is lower than 8 kJ/mol, the adsorption mechanical is physical adsorption. If E value is between 8 – 16 kJ/mol, the adsorption mechanical is chemical adsorption

Table 5.6 : Parameters used in Dubinin – Radushkevich Adsorption Isotherm calculation.

q_e (mg/g)	$\ln q_e$	ϵ^2
37.1	3.6136	38399.37
79.95	4.3814	9054.769
115.1	4.7458	4528.333
151.05	5.0176	2795.638
213.033	5.3614	1658.235
276.55	5.6224	1420.398
348.933	5.8549	1250.506
454.017	6.1181	1219.216
554.983	6.3189	1179.435
634.567	6.4529	1089.94

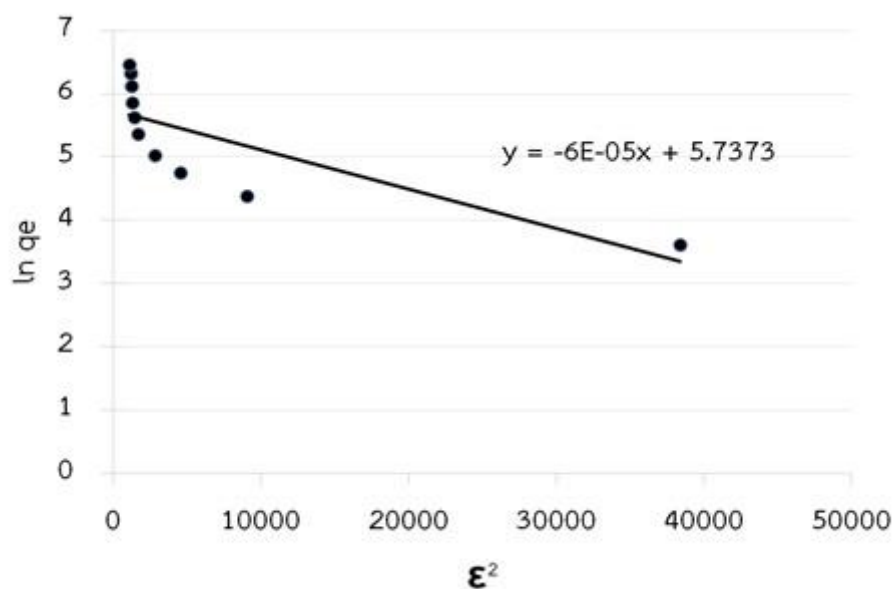


Figure 5.4 : A graph of Dubinin-Radushkevich Adsorption Isotherm.

Table 5.7 : Results from Dubinin-Radushkevich Adsorption Isotherm.

Constant	Value
$\ln q_s$	5.74
q_s (mg/g)	0.31
B_D	0.0347
E (kJ/mol)	3.79

From the Figure 5.4 and Table 5.6 and 5.7, the energy of adsorption (E) is 3.79 kJ/mol (physical adsorption). The saturation capacity (q_s) of the adsorbent type 12 is 0.31 mg/kg.

The adsorption mechanism on the adsorbent has two types. First is the physical adsorption that is the interaction between the arsenic and the adsorbent surface. The second is a chemical adsorption that is when the adsorbate reacts to adsorbent and changes the structure or chemical composition of adsorbent. From the Dubinin-Radushkevich isotherm, the energy of adsorption is 3.79 kJ/mol, which indicates that the mechanism of adsorption is physical adsorption. The physical adsorption is not necessary to use high energy. The maximum capacity of adsorbent from Langmuir adsorption isotherm is 0.45 mg/g. The value of $1/n$ from Freundlich adsorption isotherm is 1.27, indicating that the surface of adsorbent is heterogeneous.

5.3 The comparison of maximum capacity, specific surface area, and cation exchange capacity of adsorbent.

The maximum capacity is the value of adsorption ability that is the specific to each element. This study should be focused on the maximum capacity for arsenic adsorption. The cation exchange capacity (CEC) is the value of the ability that is the reaction between the ion of the adsorbent surface and the solution. This reaction is the ion exchange. The value of specific surface area is described the ability, which the adsorbent can contact the solution.

Table 5.8 : A comparison between maximum capacity, specific surface area, and cation exchange capacity of adsorbent (from ¹ Zahra et al., 2009, ² Kaufholda et al., 2010, ³ Kiviranta and Kumpulainen, 2011, ⁴ Branislava et al., 2011, ⁵ Isao and Shoichi, 1986, ⁶ ZEO INC., 2014).

Material	Max. Capacity For As(III) (mg/g)	Specific surface area (m ² /g)	CEC (cmol/kg)
Bentonite	28.2 ¹	40 – 130 ²	0.83 – 0.94 ³
Zeolite	0.97 ⁴	600 – 900 ⁵	80 – 120 ⁶
This study	0.45	32.6	10.94

From the Table 5.8, the adsorbent Type 12 has the lowest value of the maximum capacity for As. The specific surface area of our adsorbent is small (32.6 m²/g). Other geological materials such as zeolite has high specific surface area (600 - 900 m²/g) and CEC (80 – 120 cmol/kg). Bentonite is another geomaterial adsorbent , which has maximum capacity for As (28.2 mg/g) but low specific surface area (40 - 130 m²/g) and CEC (0.83 – 0.94 cmol/kg) values.

5.4 The discussion about the arsenic removal from groundwater.

From the Table 5.9, the arsenic contaminated groundwater is different in each well. A previous study by Bureau of Mineral Resources Identification and Research (2013) and Bureau of Mineral Resources Identification and Research (2014) of heavy metal contaminated in Suphan Buri and Uthai Thani, the arsenic contamination in surface water, soil and the alluvial sediment are found at the boundary of Amphoe Dan Chang in Suphan Buri and Amphoe Ban Rai in Uthai Thani. The geology of this area is contact metamorphism between granite and limestone, sedimentary rocks and metamorphic rocks such as marble and quartz-mica schist Bureau of Mineral Resources Identification and Research, 2014. This area is the potential resource of tin. The tin mine is the important source of arsenic contamination, because the associated mineral

of cassiterite such as arsenopyrite (FeAsS) is the important source of arsenic. The other source of arsenic is arsenic compounded agriculture fertilizer.

The arsenic contamination in groundwater was found in the shallow aquifers, because they contaminated with soil by arsenic compounded agriculture fertilizer. The effect of pH is the first condition to study the As contamination and the As removal. The As(V) removal was decreased with increasing pH. In addition, pH 3 is the most effectively of As(V) removal. As(III) has a maximum adsorption in the solution with pH equal to 7 (Figure 5.5). In this study, the pH values are not significant variations because the pH values of every groundwater wells were similar and assumed is the same value as the suitable condition (pH equal to 7).

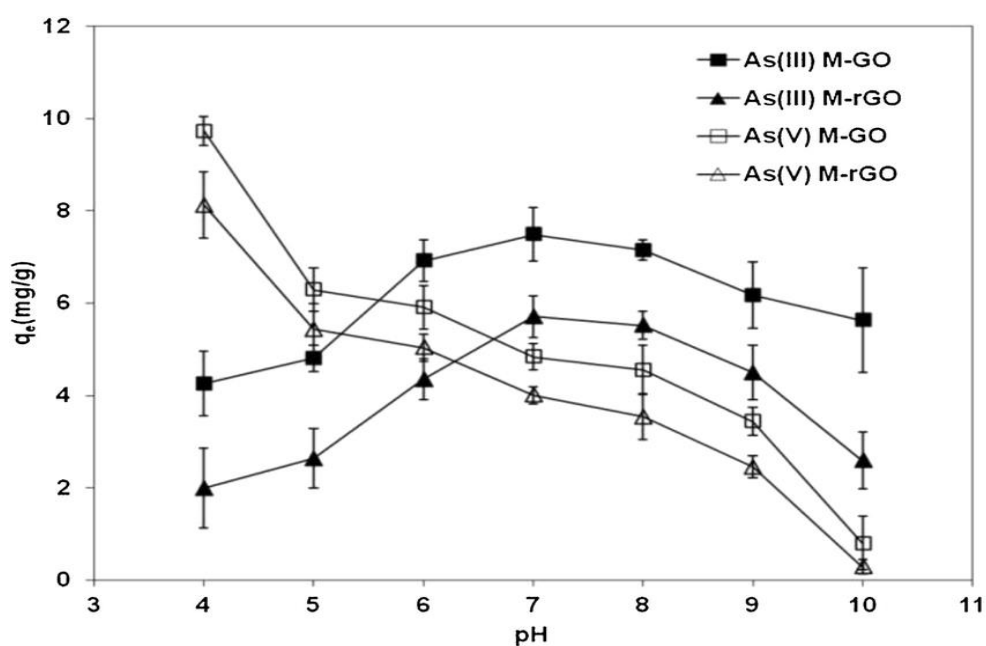


Figure 5.5 : The effect of pH on the adsorbent (after Yoon et al., 2015).

The interesting variant is the type of arsenic. The arsenic contaminated in groundwater can separate in 2 types, that are As(III) and As(V). H_3AsO_3^0 is the dominant As(III) species at pH is lower than 8, which is neutral type. At the pH is more than 8, H_2AsO_3^- is the dominant As(III) species (Figure 5.6). H_2AsO_4^- is the dominant inorganic As(V) species at pH is lower than 7, and at the pH is more than 7, HAsO_3^{2-} is the dominant As(V) species (Figure 5.7). Boyle and Jonasson (1973) suggest that As(V) is

contaminated in an oxidation phase water.

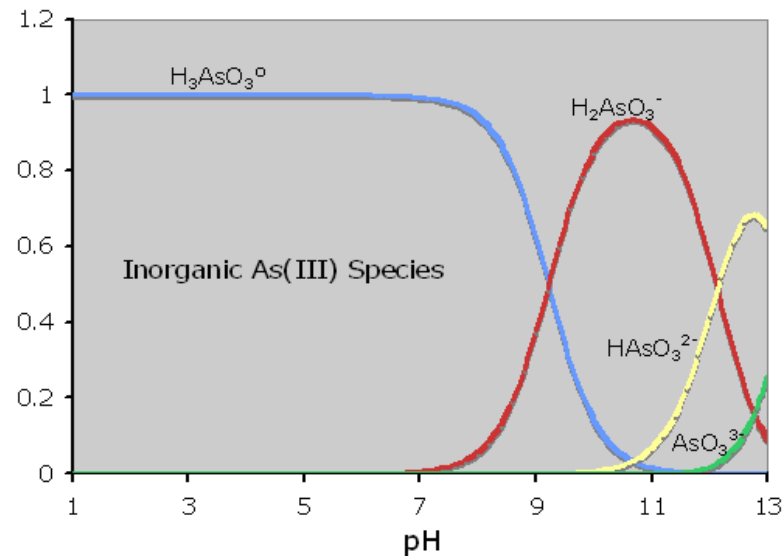


Figure 5.6 : The dominant As (III) species in the solution is controlled by pH (after Bangladesh Consortium For Arsenic Management, 2017).

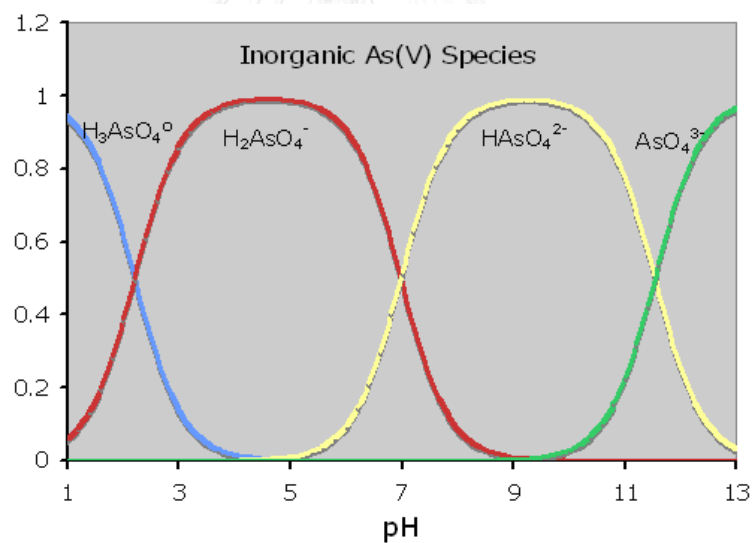


Figure 5.7 : The dominant As (V) species in the solution is controlled by pH (after Bangladesh Consortium For Arsenic Management, 2017).

The As(V) are better adsorbed than As(III) because at pH equal 6 – 8, As(V) that is negatively charged ($H_2AsO_4^-$ and $HAsO_3^{2-}$) has a stronger electrostatic than As(III) that is neutral ($H_3AsO_3^0$). Therefore As(V) are remediated better than As(III) (Jiang et al., 2013). The total dissolved solid (TDS) values may affect the adsorption capacity,

because cations and anions can react and form complex structures with the adsorbent surface. The anion that can affect arsenic removal is phosphate (PO_4^{3-}) due to its similar molecular structure as arsenate (Figure 5.8 and 5.9). Violante and Pigna (2002), reported that Al-rich mineral such as clay mineral, have a greater adsorption for phosphate than arsenate. Jain and Loeppert (2000) suggested that phosphate can effect to arsenate adsorption at the high pH as shown in and Table 5.9 (Manning and Goldberg, 1997)

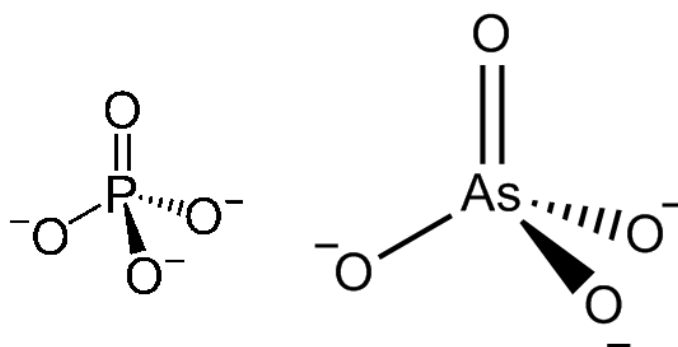


Figure 5.8 : Molecular structure of phosphate (left) and arsenate (right) (after Lee, 2013).

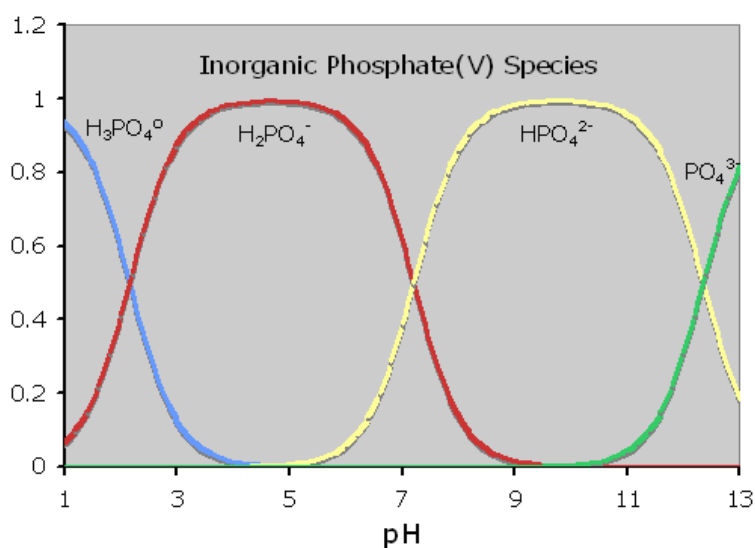


Figure 5.9 : The various species of phosphate in the solution is controlled by pH (after Bangladesh Consortium For Arsenic Management, 2017).

Table 5.9 : Arsenic and phosphate removal percentages.

Sample	pH	As (C_0) (ppb)	As (C_e) (ppb)	% As removal	PO ₄ ³⁻ (C_0) (ppm)	PO ₄ ³⁻ (C_e) (ppm)	% PO ₄ ³⁻ removal
GW01	7.15	139.33	99.67	28.46	22.56	18.61	17.51
GW02	6.95	17.10	8.60	49.71	12.87	10.54	18.10
GW03	7.05	26.24	9.39	64.21	12.86	10.32	19.75
GW04	7.25	147.00	36.30	75.31	26.98	23.96	11.19
GW05	7.18	42.67	32.00	25.01	15.51	10.74	30.75
GW06	7.03	80.33	50.33	37.35	11.82	7.52	36.38
GW07	7.16	38.70	15.20	60.72	26.87	15.26	43.21
GW08	7.01	362.30	259.00	28.51	42.53	39.34	7.50
GW09	7.25	39.67	31.67	20.71	21.91	18.94	13.56
GW10	7.35	93.80	38.20	59.28	23.89	21.76	8.92
GW11	7.08	16.13	8.08	49.91	17.43	15.55	10.79

The volumes of potassium, calcium, magnesium, and sodium increase after groundwater treatment with our adsorbent likely due to the the disintegration of adsorbents. The significant increases of potassium volumes largely affect the arsenic removal capacity. The arsenic removal percentages generally decrease after adding adsorbents (Figure 5.10 and Table 5.10).

Table 5.10 : The result of arsenic removal percentage and potassium increasing percentage.

Sample	As (C_0) (ppb)	As (C_e) (ppb)	% As removal	K (C_0) (ppm)	K (C_e) (ppm)	% K increase
GW01	139.33	99.67	28.46	3.94	41.48	951.55
GW02	17.10	8.60	49.71	6.13	14.87	142.58
GW03	26.24	9.39	64.21	2.69	10.75	299.63
GW04	147.00	36.30	75.31	9.19	21.76	136.78
GW05	42.67	32.00	25.01	2.65	39.10	1376.83
GW06	80.33	50.33	37.35	5.42	43.07	694.89
GW07	38.70	15.20	60.72	7.97	44.21	454.71
GW08	362.30	259.00	28.51	0.72	39.73	5440.68
GW09	39.67	31.67	20.71	0.59	41.20	6874.60
GW10	93.80	38.20	59.28	7.22	31.96	342.66
GW11	16.13	8.08	49.91	6.13	18.65	204.24

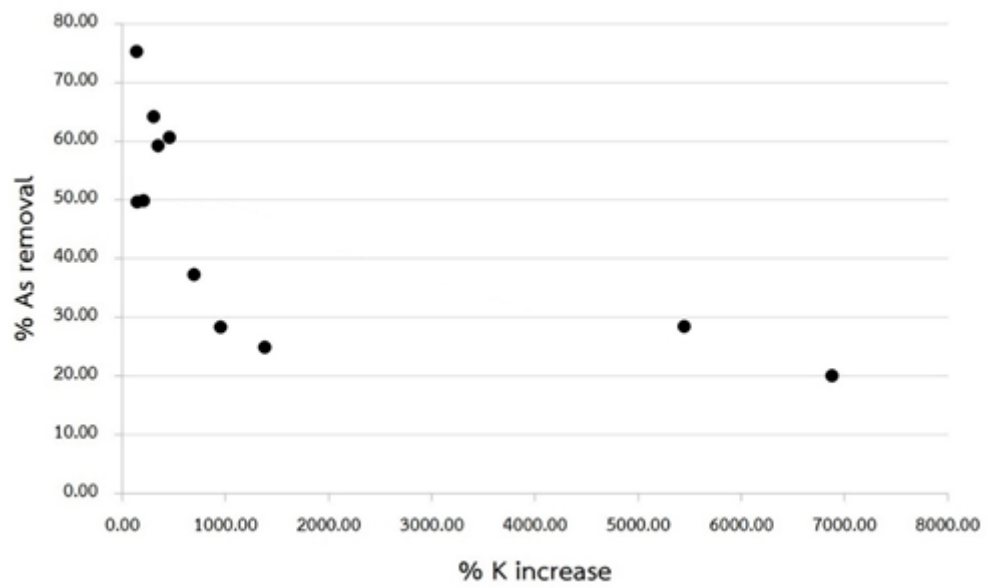


Figure 5.10 : A graph of arsenic removal percentages and the changes of potassium volumes.



CHAPTER VI

CONCLUSION

6.1 Conclusions

1. Based on XRD and XRF analyses, the geomaterial adsorbent is mainly composed of quartz, kaolinite, and iron oxide mineral such as goethite. The specific surface area is quite low at 32.6 m²/g. The adsorbent surface is heterogeneous due to high 1/n value (1.27) of Freundlich Adsorption Isotherm. In addition, SEM images show different grain sizes and shapes of adsorbents.

2. The most optimized conditions for removing As(III) is to use 10 grams of geomaterial adsorbents with a 50 ml solution in pH 7 for 2 hours. The energy of sorption is physisorption (van der waals) interpreted by the shape of the the solid – liquid distribution coefficient (K) graph that has the “unfavorable shape”. Energy of sorption value from Dubinin – Radushkevich Adsorption Isotherm ($E < 8$), it is a physisorption. The CEC value is 10.94 cmol/kg, it is very low, that show the adsorption is physisorption. The maximum capacity of this study geomaterials for As(III) removal is 0.45 mg/g.

3. The concentration of arsenic, both As(III) and As(V), are different in each groundwater well. Under the optimized conditions, our geomaterial adsorbents can remove arsenic between 20.71 – and 75.31% from contaminated groundwater wells. The variation of removal percentage is due to the abundance of phosphate, which has a similar structure to arsenic compound and may inhibit the adsorption of arsenic. In addition, some adsorbents disintegrate during treatment and release a significant volumes of potassium into water, which in turn lower the capacity of arsenic removal.

4. The cost of the adsorbent is very cheap as the price of the raw materials is low. The approximate price is 20 THB per 100 kg of adsorbents. This geomaterial adsorbent thus presents an alternative, environmental-friendly, and cost-effective method for arsenic

contaminated water treatment in Thailand.

6.2 Recommendation for future studies.

Other geological materials such as zeolite, and pumice that has high porous structure and are abundant in Thailand should be evaluated. In addition, the particle size of geomaterials should be varied and test to improve the efficiency of adsorbents. These adsorbents should be further tested with other heavy metal in contaminated groundwater to maximize the advantage of adsorbents.

The effects of cation and anion for As (III) adsorption should be studied. Because in this study, the As (III) concentration is quite small, the impact of the others cation and anion are not significant. The inorganic As contaminated groundwater is mainly composed of As (III) and As(V). The instrument that can separated the type of As is High-Performance Liquid Chromatography Inductively Coupled Plasma Mass Spectrometry (HPLC-ICP-MS).



REFERENCES

- Ahmed, F.M. 2001. An overview of arsenic removal technologies in Bangladesh and India. 19.
- Akutsu, J. 1979. On the Fossil diatoms from Amphoe Muang, Changwat Lampang, Thailand. Contributions to the Geology and Paleontology of Southeast Asia 3.
- Alkan, M., and Dogan, M. 2001. Adsorption of Copper (II) onto Perlite. Journal of Colloid and Interface Science 243: 12.
- Athikom-rangsarit, s. 1994. Arsenic contamination in Ground Water From Seven Province of Thailand. 38.
- Bangladesh Consortium For Arsenic Management. 2017. Aqueous Inorganic Arsenic. [Online]. Available from: <http://arsenic.tamu.edu/about/course/mod2/notes/pg3.htm>
- Barakat, M.A. 2011. New Trends in Removing Heavy Metals from Industrial Wastewater. Arabian Journal of Chemistry 4: 17.
- Bavornsachoti, P. 1995. Arsenic contamination in Water. Department of Mineral Resources, Thailand 33: 5.
- Boss, C.B., and Fredeen, K.J. 2004. Concepts, Instrumentation and Techniques in Inductively Coupled Plasma Optical Emission Spectrometry. 120.
- Boyle, R.W., and Jonasson, I.R. 1973. Geochemistry of arsenic and its use as indicator element in geochemical prospecting. Journal of Geochemical Exploration 2: 46.
- Branislava, M.J., Vesna, L.V., Dorde, N.V., and Ljubinka, V.R. 2011. Arsenic Removal from water using low-cost adsorbents- a comparative study. Journal of the Serbian Chemical Society 76: 16.
- Bureau of Mineral Resources Identification and Research. 2013. The Risk area from Natural Contamination, Changwat Suphanburi. 1: 174.
- Bureau of Mineral Resources Identification and Research. 2014. The Risk area from Narural Contamination, Changwat Uthai Thani. 1: 150.

- Chakir, A., Bessiere, J., Kacemia, K., and Marouf, B. 2002. A Comparative Study of The Removal of Trivalent Chromium from Aqueous Solutions by Bentonite and Expanded Perlite. Journal of Hazard Material 95: 18.
- Cheungyuesuk, N., and Suriyachai, P. 1987. Geological Survey Report : Ban Mahaphoe (5139I), Amphoe Sri Thep (5239IV), Ban Pa-niad (5139II), and Amphoe Chai-badan (5239III). 85.
- Department Mineral Resources Thailand. 2017. Kaolinite. [Online]. Available from: <http://www.dmr.go.th/main.php?filename=kaolinite>
- Department of Mineral Resources Thailand. 2007. Geological Map of Changwat Lampang. 1.
- Department of Physics Warwick University. 2010. Scanning Electron Microscopy (SEM). [Online]. Available from: <http://text.www2.warwick.ac.uk/fac/sci/physics/current/postgraduate/regs/mpags/ex5/techniques/structural/sem3>
- Department of Primary Industries and Mines Thailand. 2017. Daily Mineral Price. [Online]. Available from: <http://www.dpim.go.th/minerals-minerals/mp004.php>
- Department of Statistics Online Programs. 2017. Mixture Designs in Minitab. [Online]. Available from: <https://onlinecourses.science.psu.edu/stat503/node/61>
- Elizalde-Gonzalez, M.P., Mattusch, J., Wennrich, R., and Morgenstern, P. 2001. Sorption on Natural Solids from Arsenic Removal. Journal of Chemical Engineering 81: 187.
- Gunning, D.F. 1994. Perlite Market Study. Ministry of Energy, Mines and Petroleum Resources, Mineral Resources Division, Geological Survey Branch 97.
- Inglethorpe, S.D.J., and Pearce, J.M. 1999. Mineralogy and Petrography of Diatomite from the Lampang Basin, Changwat Lampang, Northern Thailand. 99: 29.
- Inglethorpe, S.D.J., Utha-aroon, C., and Chanyavanich, C. 1998. An Inventory of The Diatomite Deposits of The Lampang Basin, Changwat Lampang, Northern Thailand. 98: 28.
- Inglethorpe, S.D.J., Whitbread-Abrutat, P.H., and Metcalfe, R. 1999. An Investigation of the Sorption of Arsenic by Diatomite. 99: 32.

- Isao, S., and Shoichi, O. 1986. Determination of external surface areas of zeolites. Journal of Catalysis 100: 9.
- Jain, A., and Loeppert, R.H. 2000. Effect of competing anions on the adsorption of arsenate and arsenite by ferrihydrite. Journal of Environmental Quality 29: 9.
- Jalil, M.A., and Ahmed, M.F. 2001. Development of An Activated Alumina Based Household Arsenic Removal Unit. Technologies for Arsenic Removal From Drinking Water 15.
- Jiang, J.Q., Ashekuzzaman, S.M., Jiang, A., Sharifuzzaman, S.M., and Chowdhury, S.R. 2013. Arsenic Contaminated Groundwater and Its Treatment Options in Bangladesh. Journal of Environmental Research and Public Health 10: 29.
- Katsoyiannis, I., Zouboulis, A., Althoff, H., and Bartel, H. 2002. As(III) Removal from Groundwater Using Fixed-bed Upflow Bioreactors. Chemosphere 47: 8.
- Kaufholda, S., Dohrmanna, R., Klinkenbergc, M., Siegesmundd, S., and Ufere, K. 2010. N₂-BET specific surface area of bentonites. Journal of Colloid and Interface Science 349: 8.
- Kiviranta, L., and Kumpulainen, S. 2011. Quality Control and Characterization of Bentonite Materials. 102.
- Kumanchan, P., and Traiyan, A. 1986. Research on geologic environment, chemical compositions, physical properties and the uses of diatomite from the Lampang Basin, northern Thailand. 27.
- Lee, M. 2013. Arsenate and Phosphate Presentation Trans.). In 1 (Ed.),[^](Eds.), (ed., Vol. pp.). (Reprinted from.
- Liu, S. 2015. Cooperative adsorption on solid surfaces. Journal of Colloid and Interface Science 450: 15.
- Manning, B.A., and Goldberg, S. 1997. Adsorption and Stability of Arsenic(III) at The Clay Mineral - Water Interface. Journal of Environmental Science Technology 31: 7.
- Matis, K.A., Zouboulis, A., Zamboulis, P., and Valtadorou, A.V. 1999. Sorption of As(V) by Geothite Particles and Study of Their Flocculation Water, Air, and Soil Pollution 111: 297.

- Meesuk, L., and Seammai, S. 2010. The Use of Perlite to Remove Dark Colour from Repeatedly Used Palm Oil. Science Asia 36: 7.
- Mostafa, M.G., Chen, Y.H., Jean, J.S., Liu, C.C., and Lee, Y.C. 2011. Kinetics and Mechanism of Arsenate Removal by Nanosized Iron Oxide-coated Perlite. Journal of Hazardous Materials 187: 7.
- Mukherjee, A., et al. 2006. Arsenic Contamination in Groundwater: A Global Perspective with Emphasis on the Asian Scenario. Journal of Health, Population and Nutrition 24: 22.
- Nakwanit, S. 2010. Waste Management of Arsenic Accumulated Plants at Ron Phibun District, Nakorn Si Thammarat Province, Thailand. Graduated Studies Ph.D. (Biology): 171.
- Noble, R.D., and Terry, P.A. 2004. Principles of Chemical Separations with Environmental Applications. 319.
- Owen, R.B., and Utha-aroon, C. 1992. Diatomaceous sedimentation in the Tertiary Lampang Basin, Northern Thailand. Journal of Paleolimnology 22: 15.
- Pariwatawon, P. 1962. Diatomite Deposits in Changwat Lampang. 7.
- Premmanee, J., and Wijitchareamong, A. 1997. Mineral Exploration in Lumnarai Area. 191.
- Ramaswami, A., Tawachsupa, S., and Isleyan, M. 2001. Batch-mixed Iron Treatment of High Arsenic Water. Water Research 35: 6.
- Ratanasthien, B. 1992. Neogene Events Recorded in Coalfields in Northern Thailand. Development Geology for Thailand into The Year 2000 15.
- Rayment, G.E., and Higginson, F.R. 1992. Soil and Water Chemical Methods. Australian Soil and Land Survey Handbooks Series 330.
- Saisutthichai, D. 2006. Physical and Chemical Properties of Perlite and Its Application. 43.
- Sharmin, N. 2001. Arsenic Removal Processes on Trial in Bangladesh. Technologies for Arsenic Removal from Drinking Water 8.
- Silukkapatti. 2014. I-XRD-DIAGRAM1.GIF. [Online]. Available from: <https://silukkapatti.wordpress.com/2014/04/16/i-xrd-diagram1-gif/>

- Smedley, P., and Kinniburgh, D.G. 2005. Groundwater and The Environment. Essentials of Medical Geology 35.
- Tsai, W.T., Hsien, K.J., Chang, Y.M., and Lo, C.C. 2005. Removal of herbicide paraquat from an aqueous solution by adsorption onto spent and treated diatomaceous earth. Bioresour Technology 96: 7.
- Tsai, W.T., Hsien, K.J., and Yang, J.M. 2004. Silica adsorbent prepared from spent diatomaceous earth and its application to removal of dye from aqueous solution. Journal Colloid Interface Science 275: 6.
- Tsai, W.T., Lai, C.W., and Hsien, K.J. 2006. Charecterization and Adsorption Properties of Diatomaceous Earth Modified by Hydrofluoric Acid Etching. Journal Colloid Interface Science 297: 6.
- Verma, A. 2014. Graphite furnace atomic absorption spectroscopy. [Online]. Available from: <https://www.slideshare.net/AnuradhaKVerma/graphite-furnace-atomic-absorption-spectroscopy>
- Violante, A., and Pigna, M. 2002. Competitive Sorption of Arsenate and Phosphate on Different Clay Minerals and Soils. Soil Science Society of America Journal 66: 9.
- Weber, T.W., and Chakravorti, R.K. 1974. Pore and solid diffusion models for fixed-bed adsorbers. AIChE Journal 20: 11.
- Wolska, J.A., and Vrebos, B.A.R. 2004. XRF: A Powerful Oil Analysis Tool. [Online]. Available from: <http://www.machinerylubrication.com/Articles/Print/602>
- Wu, C.C., Wang, Y.C., Lin, T.F.L., and Chen, P.C. 2005. Removal of Arsenic From Waste Water Using Surface Modified Diatomite. Journal of Chinese Institute of Environmental Engineering 15: 7.
- Yoon, Y., Park, W.K., Hwang, T.M., and Kang, J.W. 2015. Comparative evaluation of magnetite-graphene oxide and magnetite-reduced graphene oxide composite for As(III) and As(V) removal. Journal of hazardous materials 304: 9.
- Zahra, N., Sheikh, S.T., Mahmood, A., and Javed, K. 2009. Removal of Arsenic From Wastewater Using Bentonite. Journal of Scientific and Industrial Research 44: 6.
- ZEO INC. 2014. [Online]. Available from: <http://zeoinc.com/ecosand/cec/>

APPENDIX

Table A1 : The variation of adsorbent amount.

Adsorbent (g)	C ₀ (ppb)	C _e (ppb)	% As removal
0.50	50.00	45.20	9.60
0.50	49.78	44.96	9.68
0.50	49.97	46.00	7.94
mean	49.92	45.39	9.08
S.D.			0.98
1.00	50.00	33.94	32.12
1.00	48.98	32.67	33.30
1.00	49.56	33.76	31.88
mean	49.51	33.46	32.43
S.D.			0.76
2.50	50.00	26.60	46.80
2.50	49.54	25.84	47.84
2.50	51.07	26.10	48.89
mean	50.20	26.18	47.84
S.D.			1.05
5.00	50.00	20.46	59.08
5.00	51.94	21.54	58.53
5.00	52.01	22.76	56.24
mean	51.32	21.59	57.95
S.D.			1.51

Table A1 : The variation of adsorbent amount (cont).

Adsorbent (g)	C ₀ (ppb)	C _e (ppb)	% As removal
10.00	50.00	4.10	91.80
10.00	51.04	4.97	90.26
10.00	50.35	4.01	92.04
mean	50.46	4.36	91.37
S.D.			0.96
25.00	50.00	0.18	99.64
25.00	48.91	0.25	99.49
25.00	49.74	0.14	99.72
mean	49.55	0.19	99.62
S.D.			0.12

Table A2: The variation of contact time.

Time (min)	C ₀ (ppb)	C _e (ppb)	% As removal
0	50.00	50.00	0.00
0	51.07	50.34	1.43
0	48.34	48.21	0.27
mean	49.80	49.52	0.57
S.D.			0.62
15	50.00	47.53	4.94
15	49.38	48.32	2.15
15	51.54	49.21	4.52
mean	50.31	48.35	3.87
S.D.			1.51

Table A2: The variation of contact time (cont.).

Time (min)	C ₀ (ppb)	C _e (ppb)	% As removal
30	50.00	44.56	10.88
30	48.24	43.02	10.82
30	49.65	44.12	11.14
mean	49.30	43.90	10.95
S.D.			0.17
45	50.00	43.45	13.10
45	51.93	44.98	13.38
45	52.87	45.59	13.77
mean	51.60	44.67	13.42
S.D.			0.34
60	50.00	37.15	25.70
60	49.87	36.64	26.53
60	50.21	37.91	24.50
mean	50.03	37.23	25.58
S.D.			1.02
90	50.00	30.18	39.64
90	51.87	31.54	39.19
90	50.67	30.07	40.66
mean	50.85	30.60	39.83
S.D.			0.75

Table A2: The variation of contact time (cont.).

Time (min)	C_0 (ppb)	C_e (ppb)	% As removal
120	50.00	1.30	97.40
120	49.43	1.27	97.43
120	50.21	1.43	97.15
mean	49.88	1.33	97.33
S.D.			0.15
150	50.00	1.00	98.00
150	48.89	0.84	98.28
150	51.47	1.32	97.44
mean	50.12	1.05	97.91
S.D.			0.43
180	50.00	0.30	99.40
180	49.93	0.47	99.06
180	51.87	0.25	99.52
mean	50.60	0.34	99.33
S.D.			0.24

Table A3 : The variation of concentration (C_0).

Concentration (ppb)	C_0 (ppb)	C_e (ppb)	% As removal
5.00	5.00	4.91	1.80
5.00	5.06	4.98	1.58
5.00	5.01	5.00	0.20
mean	5.02	4.96	1.19
S.D.			0.87

Table A3 : The variation of concentration (C_0).

Concentration (ppb)	C_0 (ppb)	C_e (ppb)	% As removal
10.00	10.00	2.92	70.80
10.00	10.54	3.01	71.44
10.00	10.32	2.90	71.90
mean	10.29	2.94	71.38
S.D.			0.55
20.00	20.00	10.72	46.40
20.00	21.97	10.64	51.57
20.00	19.98	10.84	45.75
mean	20.65	10.73	47.91
S.D.			3.19
50.00	50.00	32.68	34.64
50.00	51.97	31.97	38.48
50.00	50.21	32.54	35.19
mean	50.73	32.40	36.11
S.D.			2.08
100.00	100.00	94.10	5.90
100.00	101.21	93.87	7.25
100.00	99.65	94.29	5.38
mean	100.29	94.09	6.18
S.D.			0.97

Table A4 : The variation of pH for As concentration is 50 ppb.

Initial pH	C ₀ (ppb)	C _e (ppb)	% As removal	Equilibrium pH
3.00	50.00	27.38	45.24	2.87
3.00	50.45	26.98	46.52	2.73
3.00	51.48	28.46	44.72	2.87
mean	50.64	27.61	45.49	
S.D.			0.93	
5.00	50.00	26.67	46.66	3.24
5.00	49.92	25.91	48.10	3.15
5.00	48.37	26.47	45.28	3.21
mean	49.43	26.35	46.68	
S.D.			1.41	
7.00	50.00	26.20	47.60	5.34
7.00	50.51	25.19	50.13	5.43
7.00	50.17	25.86	48.46	5.12
mean	50.23	25.75	48.73	
S.D.			1.29	
9.00	50.00	26.44	47.12	7.63
9.00	49.18	27.95	43.17	7.32
9.00	51.76	26.12	49.54	7.45
mean	50.31	26.84	46.61	
S.D.			3.21	

Table A5 : The variation of pH for As concentration is 100 ppb.

Initial pH	C ₀ (ppb)	C _e (ppb)	% As removal	Equilibrium pH
1.00	100.00	93.17	6.83	2.12
1.00	100.65	92.56	8.04	2.24
1.00	99.67	95.34	4.34	2.32
mean	100.11	93.69	6.40	
S.D.			1.88	
4.00	100.00	72.30	27.70	3.98
4.00	100.65	75.40	25.09	3.87
4.00	99.45	70.10	29.51	4.01
mean	100.03	72.60	27.43	
S.D.			2.22	
7.00	100.00	66.30	33.70	5.25
7.00	101.76	65.89	35.25	5.18
7.00	100.45	64.56	35.73	5.17
mean	100.74	65.58	34.89	
S.D.			1.06	
10.00	100.00	68.00	32.00	9.23
10.00	97.69	67.90	30.49	9.16
10.00	99.93	66.18	33.77	9.31
mean	99.21	67.36	32.09	
S.D.			1.64	

Table A6 : The variation of contact time at pH equal to 7.

Time (min)	C ₀ (ppb)	C _e (ppb)	% As removal
30.00	20.00	17.81	10.95
30.00	19.87	18.31	7.85
30.00	20.54	18.10	11.88
mean	20.14	18.07	10.23
S.D.			2.11
60.00	20.00	17.28	13.60
60.00	21.06	17.36	17.57
60.00	20.54	17.31	15.73
mean	20.53	17.32	15.63
S.D.			1.99
120.00	20.00	14.67	26.65
120.00	19.97	14.71	26.34
120.00	20.32	15.12	25.59
mean	20.10	14.83	26.19
S.D.			0.54
180.00	20.00	16.64	16.80
180.00	19.68	16.98	13.72
180.00	21.21	16.83	20.65
mean	20.30	16.82	17.06
S.D.			3.47

Table A6 : The variation of contact time at pH equal to 7 (cont.).

Time (min)	C ₀ (ppb)	C _e (ppb)	% As removal
30.00	100.00	79.95	20.05
30.00	100.65	79.54	20.97
30.00	100.87	76.36	24.30
mean	100.51	78.62	21.77
S.D.			2.23
60.00	100.00	82.61	17.39
60.00	100.32	83.37	16.90
60.00	101.01	83.71	17.13
mean	100.44	83.23	17.14
S.D.			0.25
120.00	100.00	65.73	34.27
120.00	100.19	66.92	33.21
120.00	99.71	65.93	33.88
mean	99.97	66.19	33.79
S.D.			0.54
180.00	100.00	70.53	29.47
180.00	100.45	72.41	27.91
180.00	100.01	70.99	29.02
mean	100.15	71.31	28.80
S.D.			0.80

Table A7 : The variation of concentration at pH equal to 7.

Concentration (ppb)	C ₀ (ppb)	C _e (ppb)	% As removal
20.00	20.00	13.60	32.00
20.00	19.57	11.84	39.50
20.00	19.34	11.01	43.07
mean	19.64	12.15	38.19
S.D.			5.65
40.00	40.00	27.14	32.15
40.00	41.53	25.34	38.98
40.00	40.76	24.14	40.78
mean	40.76	25.54	37.30
S.D.			4.55
60.00	60.00	35.12	41.47
60.00	59.34	37.48	36.84
60.00	59.91	36.36	39.31
mean	59.75	36.32	39.20
S.D.			2.32
80.00	80.00	43.78	45.28
80.00	76.57	45.23	40.93
80.00	81.97	50.07	38.92
mean	79.51	46.36	41.71
S.D.			3.25

Table A7 : The variation of concentration at pH equal to 7 (cont.).

Concentration (ppb)	C ₀ (ppb)	C _e (ppb)	% As removal
100.00	100.00	61.93	38.07
100.00	102.95	62.67	39.13
100.00	101.65	56.43	44.49
mean	101.53	60.34	40.56
S.D.			3.44
120.00	120.00	66.32	44.73
120.00	120.55	65.92	45.32
120.00	119.76	63.48	46.99
mean	120.10	65.24	45.68
S.D.			1.17
140.00	140.00	70.32	49.77
140.00	139.35	71.28	48.85
140.00	140.95	67.09	52.40
mean	140.10	69.56	50.34
S.D.			1.84
160.00	160.00	72.32	54.80
160.00	161.26	69.32	57.01
160.00	160.31	69.73	56.50
mean	160.52	70.46	56.11
S.D.			1.16

Table A7 : The variation of concentration at pH equal to 7 (cont.).

Concentration (ppb)	C ₀ (ppb)	C _e (ppb)	% As removal
180.00	180.00	72.45	59.75
180.00	182.64	71.34	60.94
180.00	181.03	71.14	60.70
mean	181.22	71.64	60.46
S.D.			0.63
200.00	200.00	75.89	62.06
200.00	201.46	72.43	64.05
200.00	199.65	75.32	62.27
mean	200.37	74.55	62.79
S.D.			1.09

Table A8 : The concentrations of cation in groundwater sample before and after treatment. Treated sample is in italic and marked with an asterisk (*).

Sample	As	Ba	Be	Ca	Cd	Co	Cr	Cu	Fe	K	Mg	Mn	Na	Ni	Pb	Zn
GW01	139.3	0.05	0.00	28.67	0.00	0.00	0.00	0.02	0.04	3.94	19.38	0.01	132.63	0.00	0.00	0.21
<i>GW01*</i>	<i>99.67</i>	<i>0.07</i>	<i>0.00</i>	<i>71.02</i>	<i>0.00</i>	<i>0.00</i>	<i>0.01</i>	<i>0.01</i>	<i>0.04</i>	<i>41.48</i>	<i>30.99</i>	<i>0.61</i>	<i>154.05</i>	<i>0.00</i>	<i>0.00</i>	<i>0.02</i>
GW02	17.10	0.25	0.00	112.70	0.00	0.00	0.00	0.00	0.09	6.13	19.51	0.00	9.78	0.00	0.00	0.48
<i>GW02*</i>	<i>8.60</i>	<i>0.01</i>	<i>0.00</i>	<i>134.65</i>	<i>0.00</i>	<i>0.00</i>	<i>0.00</i>	<i>0.00</i>	<i>0.09</i>	<i>14.87</i>	<i>31.98</i>	<i>0.00</i>	<i>13.76</i>	<i>0.00</i>	<i>0.00</i>	<i>0.40</i>
GW03	26.24	0.11	0.00	67.75	0.00	0.00	0.00	0.00	0.38	2.69	23.70	0.11	19.97	0.00	0.00	0.00
<i>GW03*</i>	<i>9.39</i>	<i>0.09</i>	<i>0.00</i>	<i>108.56</i>	<i>0.00</i>	<i>0.00</i>	<i>0.00</i>	<i>0.00</i>	<i>0.40</i>	<i>10.75</i>	<i>39.53</i>	<i>0.09</i>	<i>25.87</i>	<i>0.00</i>	<i>0.00</i>	<i>0.00</i>
GW04	147.0	0.09	0.00	5.52	0.00	0.00	0.00	0.00	0.40	9.19	2.99	0.34	4.29	0.00	0.00	0.00
<i>GW04*</i>	<i>36.30</i>	<i>0.07</i>	<i>0.00</i>	<i>36.96</i>	<i>0.00</i>	<i>0.00</i>	<i>0.00</i>	<i>0.00</i>	<i>0.35</i>	<i>21.76</i>	<i>28.49</i>	<i>0.31</i>	<i>19.49</i>	<i>0.00</i>	<i>0.00</i>	<i>0.00</i>
GW05	42.67	0.07	0.00	28.94	0.00	0.00	0.00	0.01	0.22	2.65	28.44	0.12	38.45	0.00	0.00	0.06
<i>GW05*</i>	<i>32.00</i>	<i>0.08</i>	<i>0.00</i>	<i>70.60</i>	<i>0.00</i>	<i>0.00</i>	<i>0.01</i>	<i>0.01</i>	<i>0.04</i>	<i>39.10</i>	<i>37.44</i>	<i>0.33</i>	<i>63.72</i>	<i>0.00</i>	<i>0.00</i>	<i>0.04</i>
GW06	80.33	0.15	0.00	38.46	0.00	0.00	0.00	0.01	0.10	5.42	8.56	0.04	47.53	0.00	0.00	0.02
<i>GW06*</i>	<i>50.33</i>	<i>0.13</i>	<i>0.00</i>	<i>77.59</i>	<i>0.00</i>	<i>0.00</i>	<i>0.01</i>	<i>0.02</i>	<i>0.02</i>	<i>43.07</i>	<i>21.73</i>	<i>0.62</i>	<i>70.35</i>	<i>0.00</i>	<i>0.00</i>	<i>0.02</i>

Table A8 : The concentrations of cation in groundwater sample before and after treatment. Treated sample is in italic and marked with an asterisk (*) (cont).

Sample	As	Ba	Be	Ca	Cd	Co	Cr	Cu	Fe	K	Mg	Mn	Na	Ni	Pb	Zn
GW07	38.70	1.07	0.02	17.37	0.01	0.00	0.02	0.03	21.68	7.97	8.94	1.03	54.06	0.03	0.03	0.07
<i>GW07*</i>	<i>15.20</i>	<i>0.94</i>	<i>0.00</i>	<i>35.97</i>	<i>0.00</i>	<i>0.00</i>	<i>0.00</i>	<i>0.02</i>	<i>18.34</i>	<i>44.21</i>	<i>18.74</i>	<i>1.19</i>	<i>77.36</i>	<i>0.02</i>	<i>0.02</i>	<i>0.06</i>
GW08	362.30	0.12	0.00	38.51	0.01	0.00	0.00	0.02	0.04	0.72	51.24	0.02	60.73	0.00	0.00	0.04
<i>GW08*</i>	<i>259.00</i>	<i>0.12</i>	<i>0.00</i>	<i>82.23</i>	<i>0.00</i>	<i>0.00</i>	<i>0.02</i>	<i>0.02</i>	<i>0.03</i>	<i>39.73</i>	<i>57.55</i>	<i>0.61</i>	<i>89.54</i>	<i>0.00</i>	<i>0.00</i>	<i>0.02</i>
GW09	39.67	0.12	0.00	64.32	0.00	0.00	0.00	0.02	0.05	0.59	22.21	0.05	60.41	0.00	0.00	0.03
<i>GW09*</i>	<i>31.67</i>	<i>0.12</i>	<i>0.00</i>	<i>119.87</i>	<i>0.00</i>	<i>0.00</i>	<i>0.01</i>	<i>0.02</i>	<i>0.02</i>	<i>41.20</i>	<i>34.20</i>	<i>0.57</i>	<i>92.20</i>	<i>0.00</i>	<i>0.01</i>	<i>0.02</i>
GW10	93.80	0.13	0.00	30.09	0.00	0.00	0.00	0.02	0.13	7.22	5.50	0.13	24.92	0.00	0.00	0.03
<i>GW10*</i>	<i>38.20</i>	<i>0.08</i>	<i>0.00</i>	<i>78.32</i>	<i>0.00</i>	<i>0.00</i>	<i>0.00</i>	<i>0.01</i>	<i>0.12</i>	<i>31.96</i>	<i>36.07</i>	<i>0.63</i>	<i>67.98</i>	<i>0.00</i>	<i>0.00</i>	<i>0.02</i>
GW11	16.13	0.25	0.00	112.70	0.00	0.00	0.00	0.00	0.09	6.13	19.51	0.00	9.78	0.00	0.00	0.48
<i>GW11*</i>	<i>8.08</i>	<i>0.18</i>	<i>0.00</i>	<i>216.54</i>	<i>0.00</i>	<i>0.00</i>	<i>0.00</i>	<i>0.00</i>	<i>0.08</i>	<i>18.65</i>	<i>48.07</i>	<i>0.12</i>	<i>41.76</i>	<i>0.00</i>	<i>0.00</i>	<i>0.40</i>

Table A9 : The concentrations of anion in groundwater sample before and after treatment. Treated sample is in italic and marked with an asterisk sign (*).

Sample	F ⁻	PO ₄ ³⁻	Cl ⁻
GW01	1.07	22.56	109.33
<i>GW01*</i>	<i>0.84</i>	<i>18.61</i>	<i>107.33</i>
GW02	0.50	12.87	14.00
<i>GW02*</i>	<i>0.29</i>	<i>10.54</i>	<i>10.00</i>
GW03	0.70	12.86	29.00
<i>GW03*</i>	<i>0.20</i>	<i>10.32</i>	<i>25.00</i>
GW04	0.00	26.98	9.00
<i>GW04*</i>	<i>0.00</i>	<i>23.96</i>	<i>4.00</i>
GW05	0.90	15.51	52.00
<i>GW05*</i>	<i>0.63</i>	<i>10.74</i>	<i>33.33</i>
GW06	0.44	11.82	47.00
<i>GW06*</i>	<i>0.32</i>	<i>7.52</i>	<i>40.00</i>
GW07	0.60	26.87	25.00
<i>GW07*</i>	<i>0.20</i>	<i>15.26</i>	<i>21.00</i>
GW08	3.14	42.53	34.67
<i>GW08*</i>	<i>2.29</i>	<i>39.34</i>	<i>30.67</i>
GW09	0.27	21.91	114.67
<i>GW09*</i>	<i>0.25</i>	<i>18.94</i>	<i>103.33</i>
GW10	0.30	23.89	10.00
<i>GW10*</i>	<i>0.28</i>	<i>21.76</i>	<i>5.00</i>
GW11	0.50	17.43	14.00
<i>GW11*</i>	<i>0.46</i>	<i>15.55</i>	<i>11.00</i>

VITA

Miss Paveena Kitbutrawat was born on 25 October 1984 in Saraburi Province. In 2007, she graduated with a B.Sc degree from Department of geology, Faculty of Science, Chulalongkorn University. After graduation, she has been working with the Mineral Resources Analysis and Identification Division, Department of Mineral Resources, Thailand. Later on, she has decided to continue her post-graduate study leading to the M.Sc degree in Geology at Chulalongkorn University. Her major research over there was mainly focused on the Geological material for treatment of arsenic in groundwater.

